ELECTROMAGNETIC LOOPS IN ROADS FOR VEHICLE DETECTION

V. KERDEMELIDIS
University of Canterbury, Christchurch

Transit New Zealand Research Report No. 15

ISBN 0-478-04736-3
ISSN 1170-9405

P O Box 5084, Lambton Quay, Wellington, New Zealand
Telephone (04) 499-6600; Facsimile (04) 499-6666

Kerdemelidis, V. 1993. Electromagnetic loops in roads for vehicle detection. *Transit New Zealand Research Report No. 15.*

Keywords: electromagnetism, electromagnetic loop, feeders, roads, traffic, vehicles, vehicle detection

AN IMPORTANT NOTE FOR THE READER

While this report is believed to be correct at the time of publication, Transit New Zealand and its employees and agents involved in preparation and publication cannot accept any contractual, tortious or other liability for its content or for any consequences arising from its use and make no warranties or representations of any kind whatsoever in relation to any of its contents.

The report is only made available on the basis that all users of it, whether direct or indirect, must take appropriate legal or other expert advice in relation to their own circumstances and must rely solely on their own judgement and such legal or other expert advice.

ACKNOWLEDGMENTS

New Zealand National Roads Board, now Transit New Zealand, provided the stimulus and funds for this investigation.

Australian Roads Research Board gave permission to reproduce Figure 3.13.

Dr A.J. Nicholson, University of Canterbury, for continued encouragement and advice, David Silvester and traffic engineers of Transit New Zealand for support, Hardings Signals for supplying equipment for some of the measurements.

CONTENTS

ABSTRACT

Experimental and theoretical studies of the properties and performance of electromagnetic loops and feeder lines used in road vehicle detection systems were carried out to determine causes of erratic behaviour of loops, and to improve their performance.

Basic concepts and terminology of loops are introduced and the effects of objects in their proximity are studied. The magnetic flux density distributions near rectangular and quadrupole loops are analysed, assuming the loops to be in free space or away from other objects that may affect their magnetic fields. Magnetic flux density distribution for a quadrupole loop is compared with published measured spatial sensitivity for the same type of loop. The comparison indicates a strong correlation between spatial sensitivity of a loop, defined as the relative change in loop inductance caused by an object's presence, and its magnetic flux density distribution. From these findings, optimum loop sizes that give maximum sensitivity to conducting sheets are determined using horizontal plane sheets to simulate a vehicle's underside such as of a car or truck, and vertical conducting sheets to model motorcycles and bicycles.

The effects of various types of feeders (or transmission lines) on the sensitivity of the loop-feeder system are defined and an analytical expression for the sensitivity is derived. A relationship exists between the value of the loop reactance and the feeder characteristic impedance that reduces the adverse effects of the feeder length.

The effects of conducting screens (slabs, steel reinforcing in concrete, etc.) on loop performance are also investigated both analytically and experimentally using models. Again, the results show excellent agreement in that the sensitivity of a loop is reduced dramatically by the presence of conducting objects, although ferromagnetic materials do not seem to have such a great effect as non-ferromagnetic materials.

1. INTRODUCTION

The motivation for this study arose from discussions with Dr Alan Nicholson, Department of Civil Engineering, University of Canterbury. Reports that vehicle detection systems often behave in an erratic manner suggested that their operation needed to be investigated with the view to possibly improving their performance. Thus the loop-detector combinations of a number of vehicle detectors were observed with the loops above ground, i.e. not cut into a road surface, taking into consideration the limitations of this experimental approach.

The erratic behaviour of the complete system was difficult to determine and the problem was further compounded by the nature of the chips contained in the electronic detectors. These were proprietary chips, being specially developed for the company and for which no data could be obtained. Thus, only the three main accessible components:

loop or front end of the sensing system,
feeder or connecting link between the sensor and electronic detector, and the
proprietary electronics,

were investigated to determine the properties of loops and the effects of feeder on the sensitivity of the system operation.

The properties of loops have been experimentally investigated extensively by workers in other parts of the world but especially in Australia by the Department of Main Roads, New South Wales. This analytical study has been designed to complement these earlier investigations and to give greater insight into the properties of loops when they are used as vehicle sensors. The study is also designed to clarify a number of problem areas associated with the operation of loops, and to decide if the mathematical models can be used to theoretically predict the suitability of a loop configuration for detecting vehicles on roads.

2. THEORY

2.1 Basic Electromagnetic Theory

A conductor carrying an electric current creates a magnetomotive force "mmf". For a wire element "dℓ" metres long and carrying a current of "I" ampere, the elemental mmf is:

$$dH = \frac{I.d\ell.\sin\theta}{4\pi R} \; Amps$$

(Equation 2.1)

where: "θ" is the angle between the direction of the current element and the point in space where the "mmf" is measured, and

"R" is the radial distance from the centre of the element "dℓ" to the field point.

The "mmf" is a vector quantity. Its direction is given by the right-hand screw about the direction of the conventional current flow. The mmf lines form concentric curves.

The total field, "H", from the current elements is related to the flux density, "B", a quantity defined by:

$$\vec{B} = \mu\vec{H} \qquad \text{(Equation 2.2)}$$

where: "μ" is a constant for a linear medium.

A related quantity is the total flux ,"ϕ", defined by the integral of the flux density over the area of interest,

$$\phi = \int_{AREA} \vec{B}.\vec{ds} \qquad \text{(Equation 2.3)}$$

Note: If the area is fixed, then the (total) flux "ϕ" is proportional to the flux density over the area.

For a magnetic circuit the equivalent of Ohm's Law is the equation:

$$Flux = \frac{mmf}{Reluctance} \qquad \text{(Equation 2.4)}$$

Here, "Reluctance" is magnetic impedance. Reluctance of non-magnetic materials is close to that of a vacuum and reluctance of paths through linear ferromagnetic materials is less than through the air. Hence (by Equation 2.4) the flux will be greater through a ferromagnetic material than in free space.

2.2 Loops

If the wire carrying the current is shaped into a closed loop, then "mmf" shown as magnetic lines are as shown in Figure 2.1.

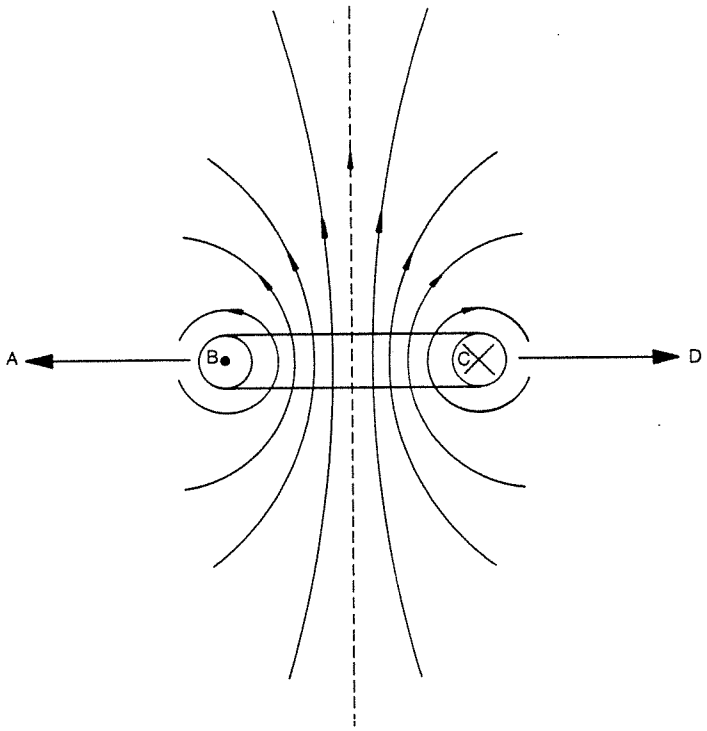

Figure 2.1.
Magnetic field lines
surrounding loop current.

B-C loop wire

Note, by the corkscrew rule, the fields from each conductor **add inside** the loop, i.e. between B and C, because the mmf lines point in the **same** direction. In contrast, the fields outside the loop, i.e., between A(= $-\infty$) and B and also between C and D(= $+\infty$) are the difference between the fields of the two conductors forming the loop. This is the reason why the magnetic fields are stronger inside the loops and fall off rapidly outside (in the plane) of the loop.

2.3 Objects Near Loops

A conductor in a time-changing magnetic field will have an electromotive force (emf) induced in it. The change in the magnetic field may be caused by:

1. The motion of the conductor in a magnetic field. The field itself may be space- or time-invariant or both, or

2. A time-varying magnetic field even if the conductor is stationary.

Effect in (1) may be called "motional" emf and the effect in (2) the "transformer" emf. Thus, in general, the total emf on a conducting object near a loop is:

$$E = \left[-\frac{\partial \phi}{\partial t}\right] \textit{Time varying field} + \left[-\frac{\partial \phi}{\partial t}\right] \textit{Motion in the field}$$

(Equation 2.5)

where: ϕ is the total flux intercepted by the object (Equation 2.3).

This emf (Equation 2.5) causes currents to flow through the conductor. The magnitude of the currents depends on the time rate of change of flux through the object, its conductivity and geometry.

The **total flux** through an object depends on its:

1. Size,
2. Material,
3. Flux density at the object.

In Equation 2.5, the first term is a function of the time-rate of flux change. If the time variation is sinusoidal, then this term is proportional to the frequency of the magnetic field, i.e. the loop-excitation current.

The second term in Equation 2.5 depends on the speed at which the object moves across the field to cause the change in flux with time. The resultant currents in the conductor depend on its geometry and material. The important parameters in the induction of currents in conducting objects in a magnetic field are:

1. Flux density at the object,
2. Relative size of the object and its aspect, relative to the field and its geometry,
3. Frequency of operation,
4. Rate and direction of motion of the object relative to the magnetic field.

2.4 Loops

2.4.1 Self Inductance

A parameter which is a function of a loop's geometry is the loop "self inductance", "L", defined as:

$$L = \frac{Total\ Flux\ Through\ Loop}{Current\ in\ the\ Loop\ Wire}$$

(Equation 2.6)

2.4.2 Conductor Near a Loop

A conducting object near a loop will have circulating or eddy currents induced on it if there is a relative motion between the object and the field or because of the alternative nature of the loop excitation (or both) (Equation 2.5). The induced currents have magnetic fields associated with them. These fields react with the original loop fields.

Conductive objects tend to reduce the total flux through the loop. Equation 2.6 shows that this reduction will result in a decrease in the self-inductance, "L", of the loop relative to its free space value.

2.4.3 Ferromagnetic Materials

When magnetising materials, such as iron or steel, are introduced near a loop, the reluctance (Equation 2.4) of the magnetic circuit decreases. This causes an increase in the total flux through the loop, relative to its free-space value. From Equation 2.6, this will result in an increase in the loop self inductance.

Note that the overall effect on flux through the loop, and therefore on the loop inductance caused by an object, depends on its geometry and the relative contributions of the conductor (or eddy) currents and of its magnetic (reluctance) properties.

2.4.4 Loop Sensitivity

If the initial value of the loop self inductance is "Lo" and its self inductance with an object present is "L", then the loop "sensitivity" is defined as:

$$Loop\ sensitivity = \frac{L-L_o}{L_o} = \frac{\Delta L}{L_o}$$

(Equation 2.7)

where "$\Delta L = L - L_o$" is the **change** in loop self inductance caused by the presence of the object.

Note that since the loop sensitivity to an object's presence depends on the relative amount of the flux that the object intercepts, it follows that the locations of high flux densities will be high sensitivity areas. This is because an object of a **given** size will intercept a proportionately greater amount of total flux in a high flux density location than in a low density one.

Such reasoning leads to investigating the effects of an object in the form of a flat conducting slab, i.e.:

> "Given the height and the size of the object or slab above a loop, is there a loop size that maximises the flux density at the height of interest?"

If such an optimum loop size does exist, this will provide maximum sensitivity for the objects at the height of interest.

In Section 4, the distribution of the (vertical) magnetic flux density in single loops is investigated theoretically. This flux density is normal to the loop plane and to the assumed object's surface.

The above assumption implies that the effect of the motor vehicles (cars, vans and trucks) may be modelled by a plane conducting slab and experiments have established its validity.

2.5 Analysis

For simplicity, the study of the flux density distribution is confined to the vertical component of the magnetic flux density through the centroid of rectangular and circular loops.

The vertical component of the magnetic flux density at a height "z" metres above a single-turn circular loop of diameter "a" metres, is given (Popovic 1971) as:

$$B_z = \left[\frac{\mu_o I}{2\pi}\right] \frac{\pi a^2}{(a^2 + z^2)^{3/2}} \; tesla$$

(Equation 2.8[1])

The vertical flux density at a height "z" metres above a rectangular loop of "2a" metres by "2b" metres dimensions is:

$$B_z = \left[\frac{\mu_o I}{4\pi}\right] \frac{2ab}{(a^2 + b^2 + z^2)^{1/2}} \left[\frac{1}{a^2+z^2} + \frac{1}{b^2 + z^2}\right] \; tesla$$

(Equation 2.9)

"B_z" is measured along a line perpendicular to the centroid of the loop.

From Equation 2.9, the corresponding (i.e. along the centroid) flux density at a height "z" above a square loop with side dimensions "2a" metres is:

$$B_z = \left[\frac{\mu_o I}{4\pi}\right] \frac{4a^2}{(z^2 + a^2)(2a^2 + z^2)^{1/2}} \; tesla$$

(Equation 2.10)

Equations 2.8 and 2.10 tend to zero for $a \to 0$ and $a \to \infty$. Thus, stationary points are expected in the range $0 < a < \infty$.

Circular loop: For a given current and number of turns the maximum axial magnetic flux density at a height "z_o" occurs when the radius "a" of the loop is:

$$a_o = \sqrt{2}\, z_o$$

a_o and z_o are in the same units (metres)

(Equation 2.11)

---

[1]T = tesla, SI unit of magnetic flux density (1 weber magnetic flux/m^2)

Rectangular loop: From Equation 2.10 for a given current "I", the vertical flux density at a height "z_o" on a line through the centroid of a square loop of "2a x 2a" dimensions is **maximum** when "a= a_o" where:

$$a_o = \frac{\sqrt{2}}{\sqrt{5-1}} z_o$$

(Equation 2.12)

2.6 Results

Graphs showing the variation of the vertical flux with height above loops are given in Figures 2.2 to 2.7. The height is measured along a perpendicular through the centroid of the loop. Note that the vertical co-ordinate in **all** graphs is the vertical magnetic flux density component. All co-ordinates are drawn with the **same vertical scale**.

Results in Figures 2.2 to 2.4 indicate that high flux densities are achieved at low heights, i.e. close to the loop surface, for narrow rectangular loops (Figure 2.3). However, for narrow loops, the flux density drops off with height more rapidly than for wider loops.

Figures 2.5 to 2.7 show the flux density at a few selected heights. The results indicate that **optimum** loop dimensions exist for each height.

From these analytical results the conclusion is that when loops are used to detect objects at a number of different heights, e.g. cars and trucks, then either

1. a compromise rectangular loop must be used, or

2. a number of loops be used, optimised for a number of the most commonly occurring vehicle-chassis heights.

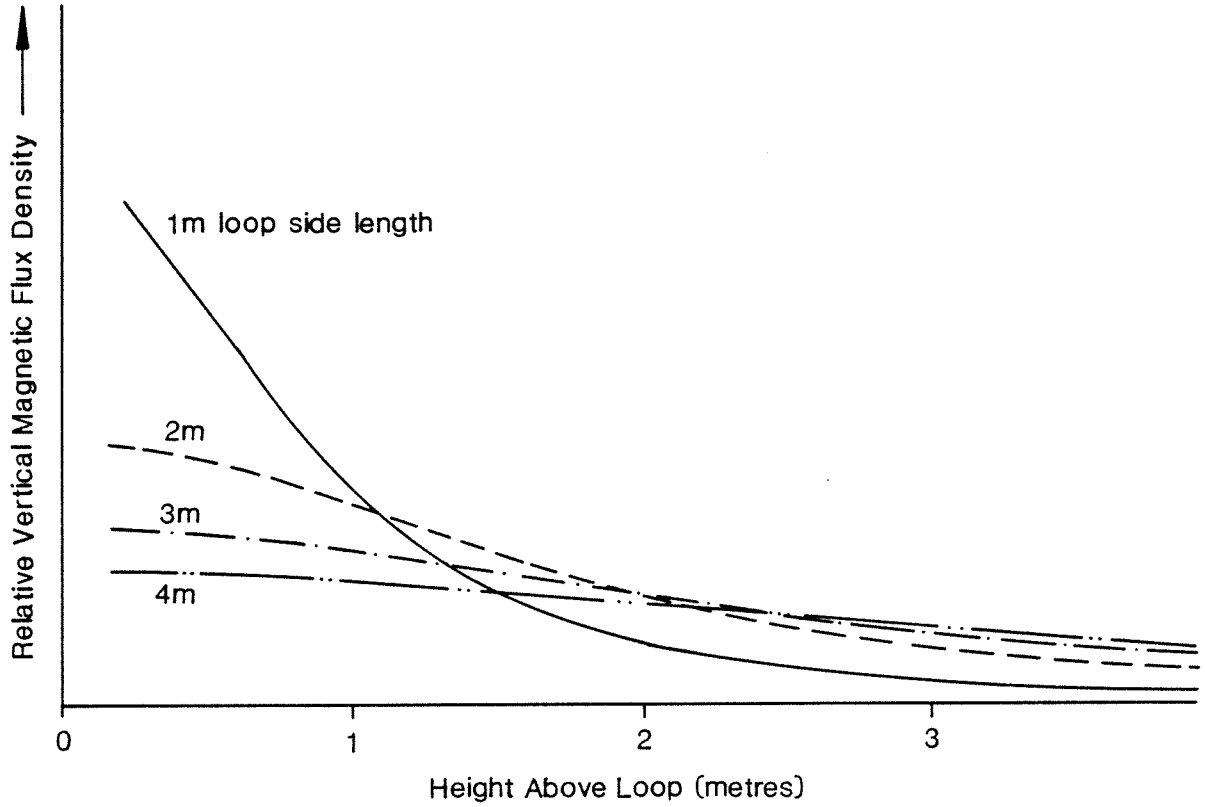

Figure 2.2. Square loops: vertical magnetic flux density along the normal to the loop plane at the loop centroid. The parameter is the length of the loop side at 1, 2, 3 and 4 metres.

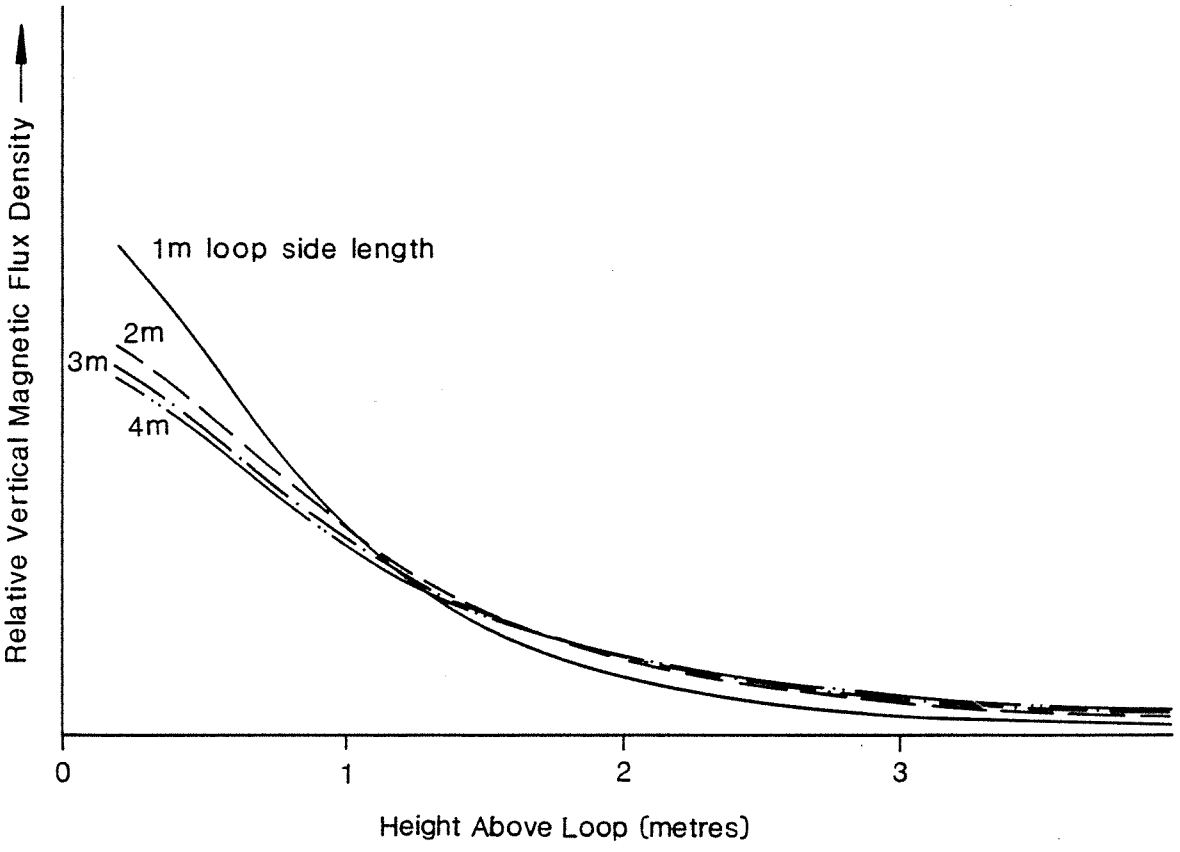

Figure 2.3. Rectangular loops: vertical magnetic flux density along the normal to the loop plane at the loop centroid. Two sides of the loop are fixed at 1m length, the parameter is the length of the other two sides which are variable at 1, 2, 3 and 4 metres.

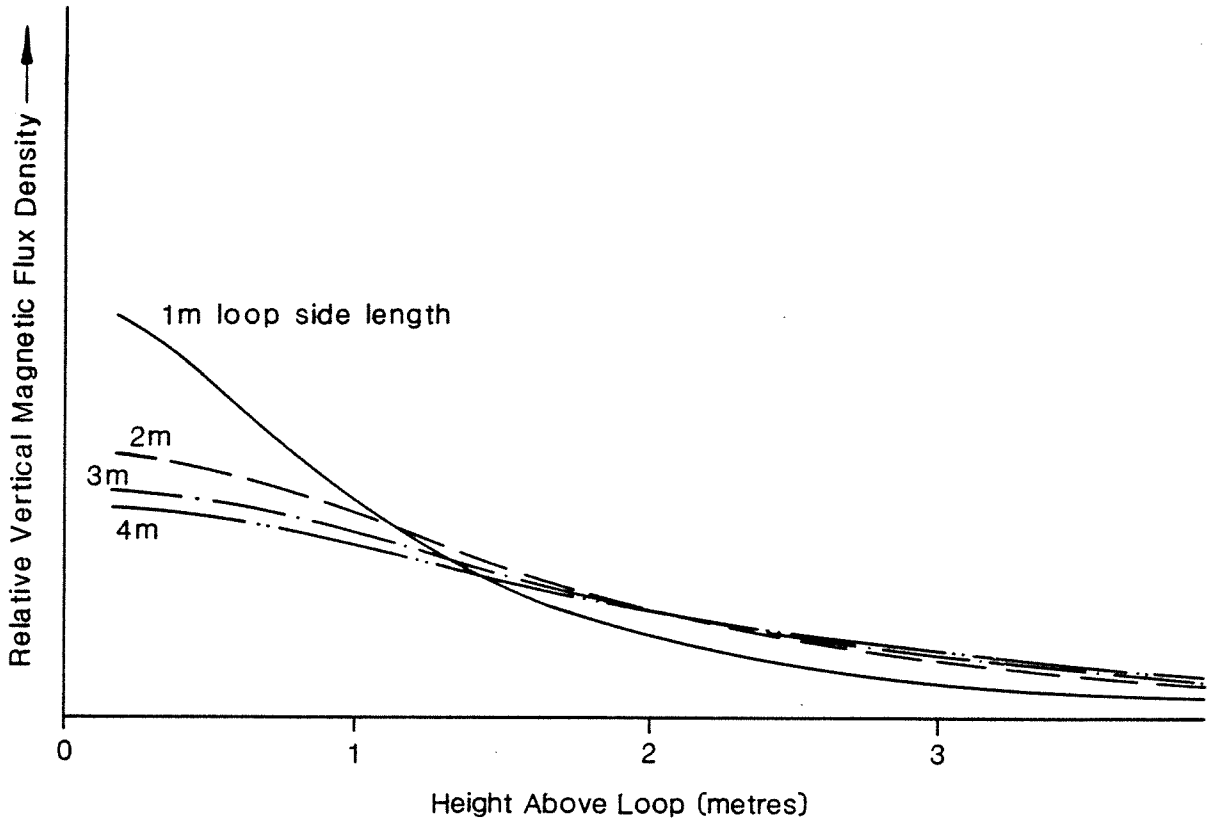

Figure 2.4. Rectangular loops: vertical magnetic flux density along the normal to the loop plane at the loop centroid. Two opposite sides of the loop are fixed at 2m length, the parameter is the length of the other two sides which are variable at 1, 2, 3 and 4 metres.

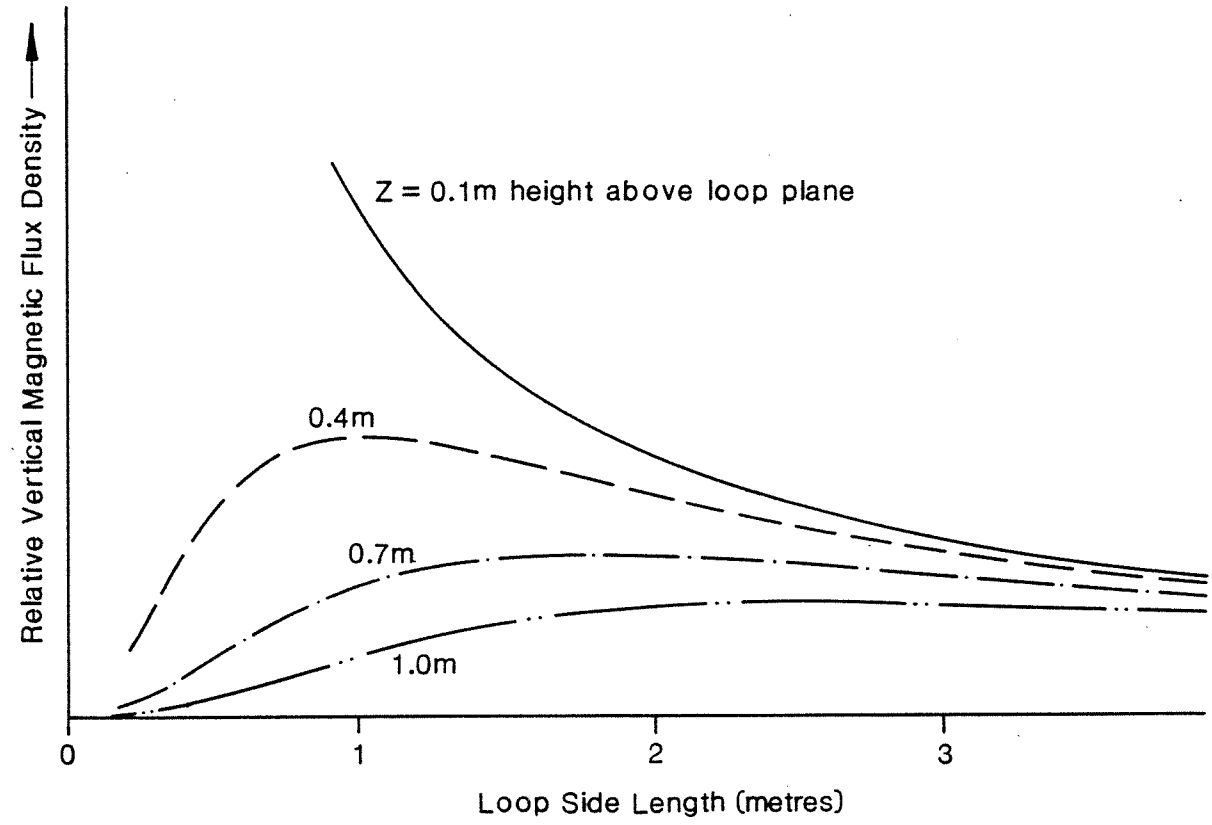

Figure 2.5. Square loops: vertical magnetic flux density along the centroid of the loop as function of loop (square) side length. The parameter is the height "z" above the loop, with z = 0.1, 0.4, 0.7 and 1.0 metres.

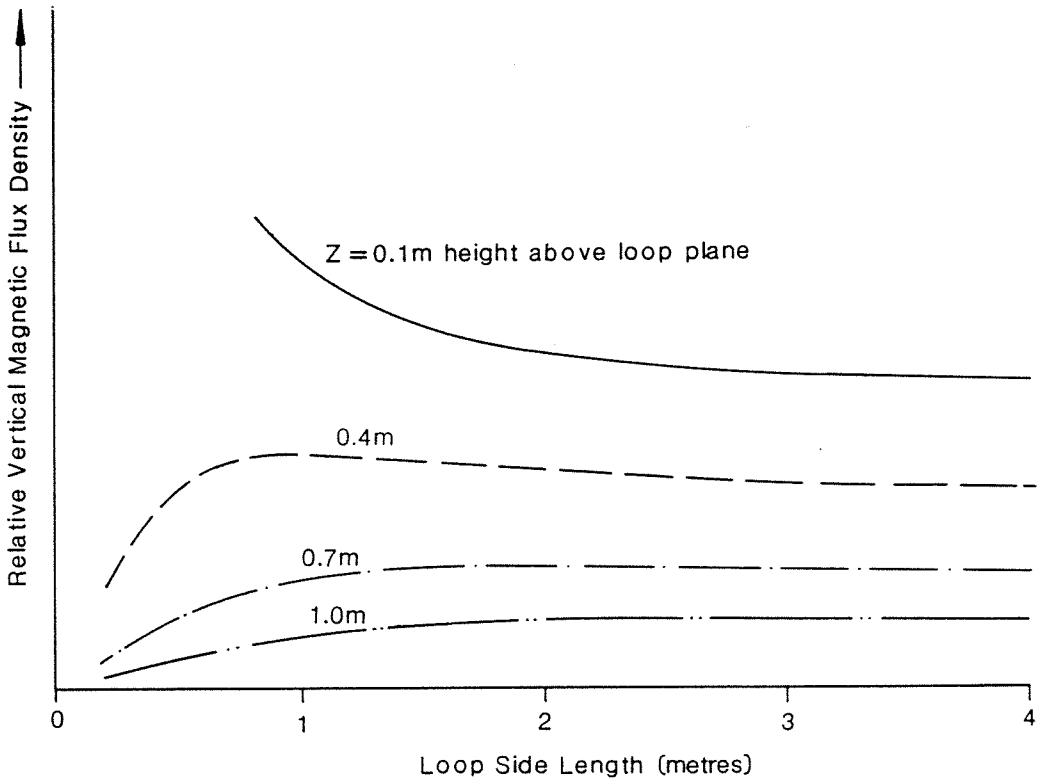

Figure 2.6. Rectangular loops: vertical magnetic flux density along the centroid of the loop as function of loop side length. Two opposite sides of the loop are fixed at 1m length, the other two sides are variable. The parameter is the height "z" above the loop plane, with z = 0.1, 0.4, 0.7 and 1.0 metres.

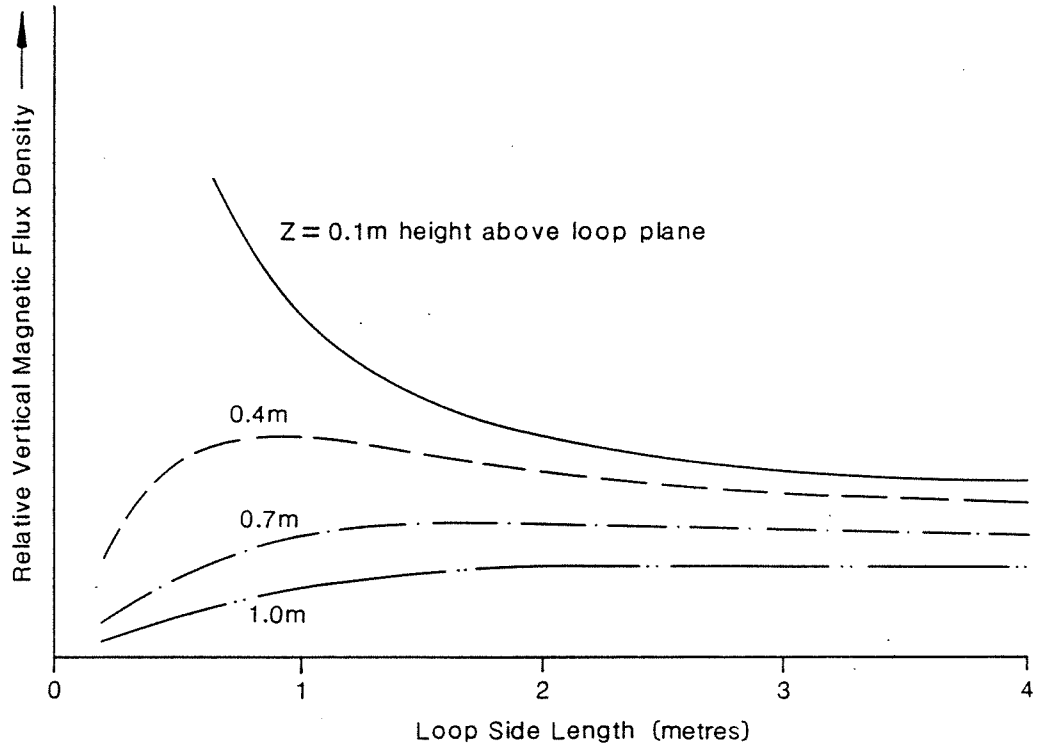

Figure 2.7. Rectangular loops: vertical magnetic flux density along the centroid of the loop as function of loop side length. Two opposite sides of the loop are fixed at 2m length, the other two sides are variable. The parameter is the height "z" above the loop plane, with z = 0.1, 0.4, 0.7 and 1.0 metres.

3. A MATHEMATICAL MODEL & RESULTANT SPATIAL DISTRIBUTION OF MAGNETIC FLUX DENSITY OF VARIOUS LOOPS

3.1 Introduction

Road loops are widely used for traffic management. They are a link in the monitoring system and any increased understanding of their characteristics may help improve the overall system performance. In Sections 3.2 and 3.3, mathematical models of two types of loops are formulated and used to study the magnetic flux density distributions in space. The formulation is based on the assumptions that the currents are concentrated in thin, "mathematical" lines.

3.1.1 Rectangular Loops

These loops are considered, assuming free space conditions and no current interaction (i.e. line current assumption) among the various elements of the loop. Magnetic vector potentials, caused by currents, are derived and the magnetic flux densities are then determined by the "curl" vector operation. Separate expressions for the vertical and horizontal (relative to the loop plane) magnetic flux densities are derived. These expressions are used to compute the flux components shown in various figures.

3.1.2 Quadrupole Loops

A similar procedure is followed to obtain the fields of quadrupole loops. Finally, and most importantly, a composite graph of vertical and horizontal([2]) (or cross-) field densities is computed and compared with the observed loop sensitivity data for a quadrupole loop.

3.2 Mathematical Formulation

3.2.1 Magnetic Vectors

The magnetic flux density caused by loop currents is determined first by finding the magnetic vector potentials of the currents. The magnetic flux density, B (a vector quantity), is related to the magnetic vector potential by:

$$\vec{B} = \nabla \times \vec{A} = CURL\ \vec{A}$$

(Equation 3.1)

---

[2] "Horizontal" flux density refers to flux density directed parallel to the loop plane. "Cross-field" flux density is **also horizontal** but is specifically directed across and not along the road lane.

This procedure simplifies the work considerably. The vector magnetic field caused by a current of I ampere in a filamental conductor in the direction "$d\vec{s}$" is given by:

$$\vec{A} = \frac{\mu I}{4\pi} \int \frac{d\vec{s}}{r} \qquad \text{(Equation 3.2)}$$

where μ is a material constant; for free space, $\mu = \mu_o = 4\pi \times 10^{-7}$ henry. m^{-1}, and r is the distance from d $\vec{s}$ to the field point. Equations 3.1 and 3.2 and the operations they define are explained in Langmuir (1961, p. 72).

3.2.2 Rectangular Loops

Figure 3.1 shows the geometry of a loop. The traffic flow is in the x - direction and the y-z plane is the midsection of the loop at x = 0. For a rectangular loop, the current flow is in directions ABFCDEA. (For the quadrupole case the currents flow in a "figure of 8" form along ABFEDCFEA.) Note that the currents are reversed for quadrupole and rectangular loops in section DC. The current in the middle conductor EF (of the quadrupole) is twice that of the side conductors BA and CD. With the current of magnitude I ampere and in directions shown, the magnetic vector potential component "Ax" at the field point "f(x,y,z)" is found from:

$$A_x = \frac{\mu I}{4\pi} \left[\int_{-xo}^{xo} \frac{dx^1}{r^-} - \int_{xo}^{-xo} \frac{dx^1}{r^+} \right] \qquad \text{(Equation 3.3)}$$

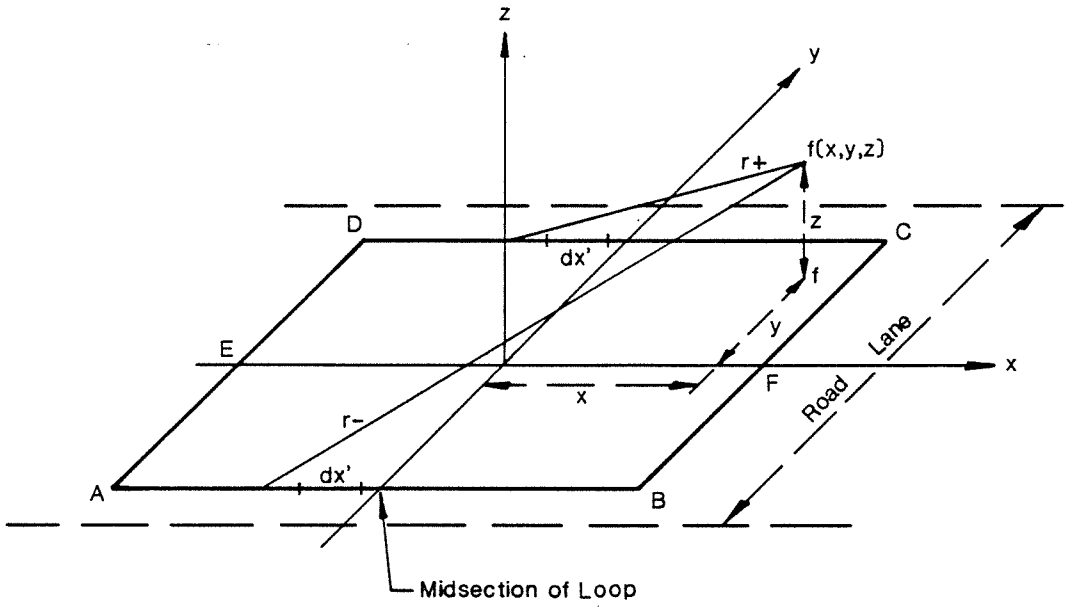

Figure 3.1. Geometry of a loop. All angles are 90°. Loop ABCDA is a rectangular loop if sides AB = CD ≠ BC = DA. If AB = CD = BC = DA, the loop is a square. If the loop includes the side EF, then loop ABFEDCFEA is a quadrupole. It can be a square or a rectangular quadrupole.

A similar integral expression may be written for the y-directed magnetic vector component.

Using the components "A_x" and "A_y" of the magnetic vector, the magnetic flux density vector can be determined from Equation 3.1:

$$\vec{A} = \vec{ex}\, A_x + \vec{ey}\, A_y$$

(Equation 3.4)

where "ex" and "ey" are unit vectors in x- and y- directions respectively, and the component "A_z" is zero since there is no z-directed current. Equation 3.4 gives the resultant magnetic vector of a loop in free space.

3.2.3 Quadrupole Loops

A quadrupole loop is, effectively, made up of two rectangular loops wound in opposite directions so that the currents, in the sides that coincide (EF) to form the quadrupole loop, flow in the same direction. Thus the current in the middle conductor is twice that of the outside conductors. This explains the **skewed** vertical magnetic field observed in Figures 3.5 and 3.6.

This type of loop is called a quadrupole because a single loop produces a dipole type of magnetic field, while the two equivalent loops in quadrupole loops give rise to a resultant field of **two** dipoles.

3.3 Computational Results

Numerical results were obtained for rectangular and quadrupole loops using Equation 3.1 and the appropriate magnetic vector components. Vertical and horizontal (transverse to the lane, i.e. in the y-z plane) magnetic flux densities were computed for single turn loops.

Figures 3.2 to 3.4 are for a 2m x 2m rectangular (square) loop. Graphs in Figures 3.2 and 3.3 show spatial distributions of vertical magnetic flux densities at heights 0.25m and 0.50m, respectively. A 2m x 2m square loop is optimum for detecting horizontal (conducting) slabs at a height of 0.786m. Figure 3.4 gives the horizontal (transverse) flux density at 0.40m above the loop plane.

Graphs in Figures 3.5 to 3.7 are for a 2m x 2m quadrupole. Figures 3.5 and 3.6 give the vertical flux densities above the loop at heights of 0.20m and 0.50m above it. Figure 3.7 depicts the spatial horizontal distribution of flux density for the quadrupole.

Graphs in Figures 3.8 to 3.11 show flux density profiles at midsections (x = 0, Figure 3.1) of rectangular and quadrupole loops. Figure 3.12a is a composite; it depicts both vertical and horizontal flux density profiles through the midsection of a quadrupole. The heights at which the fields were computed for this graph, were chosen so that each corresponds to the "mean" height for a particular type of vehicle. This was to allow comparison with observed sensitivity results for a similar type of loop (quadrupole) (Figure 3.13) (Morris *et al.* 1978).

To find representative heights of various types of vehicles, measurements were made of chassis heights of cars, motorcycles and trucks. Typically, the chassis of a private car above the road surface was in the range 0.20m to 0.30m. The corresponding height for a range of trucks was about 0.85m. Because of their construction it is considered that a horizontal conducting slab at the appropriate heights may be used to model the cars and trucks.

Because of their construction, motorcycles may be considered as vertical conducting slabs. Measurements on a representative selection of motorcycles gave, as their centroid, a height of about 0.40m above the road surface.

Thus, the composite flux density graph (Figure 3.12a) has two vertical flux density plots at 0.25m (for cars) and at 0.85m (for trucks) and the horizontal (cross) field is computed at a height of 0.40m (for motorcycles).

In Figures 3.14 and 3.15 the widths (across the road lane) of the quadrupole loop were kept constant at 2m and the length was varied from 0.5m to 3m. The resultant **vertical magnetic flux density** profiles at 0.40m above the loop are plotted in Figure 3.14. This shows that there is little increase in the field after the quadrupole becomes more than two juxtaposed squares of 1m x 1m. Thus for a width of "2B" metres, the length of the quadrupole loop need not exceed "B" metres.

When the **cross-lane field** is considered (Figure 3.15), a loop of 2m width (across lane) the cross-field increases with loop length but the **rate** of flux increase drops off rapidly past the loop length of 1m. As for the case of the vertical flux (Figure 3.14), the optimum size of a quadrupole loop is 2m x 1m. For a loop length greater than 1.75m, no perceptible increase in cross-field was noted. Thus the optimum size for car and motorcycle detection is a loop of 2m x 1.75m.

3.4 Summary

Even though Figure 3.13 is a linear-log plot, the similarities between the flux density curves of Figure 3.12a and the corresponding experimental sensitivities (Figure 3.13) for the various types of vehicles are striking. A linear-log version (Figure 3.12a) has been made of Figure 3.12a to show the close similarities between flux densitiy curves and experimental sensitivities (Figure 3.13). The positions of maximum flux densities and maximum sensitivities are on the linear axes and thus not affected by the transformations.

Clearly a strong cross-field magnetic flux density at a height of about 0.40m right across each of the road lanes is essential if motorcycles are to be detected with any reasonable certainty. In comparing the curves in Figures 3.12a and 3.12b with Figure 3.13, note that the sensitivity curves (Figure 3.13) tend to be smoothed-out versions of the flux density curves because the finite width of the vehicles gives a running **average** of the flux density curve. This result gives confidence to use loop models in the development of loop configurations to match the expected traffic. It becomes apparent now that quadrupole loops provide a cross-field structure more suitable for motorcycle traffic than do the square loops.

A possible solution for detecting cars, trucks and motorcycles may be provided by combinations of a square loop and a quadrupole loop. The two could be staggered to provide an almost continuous cross-field in each lane. The dimensions of the square loop would be optimised to detect trucks and the quadrupole loops would be optimised to detect cars. The combination of the two would provide the required cross-field to detect motorcycles. Thus 2m x 2m square loop combined with a 2m x 1.75m quadrupole with the two staggered in-lane by 0.50m (relative to each other) would provide vertical fields to detect vehicles in (chassis) height range from 0.25m to 0.85m and a resultant relatively continuous cross-field to detect motorcycles.

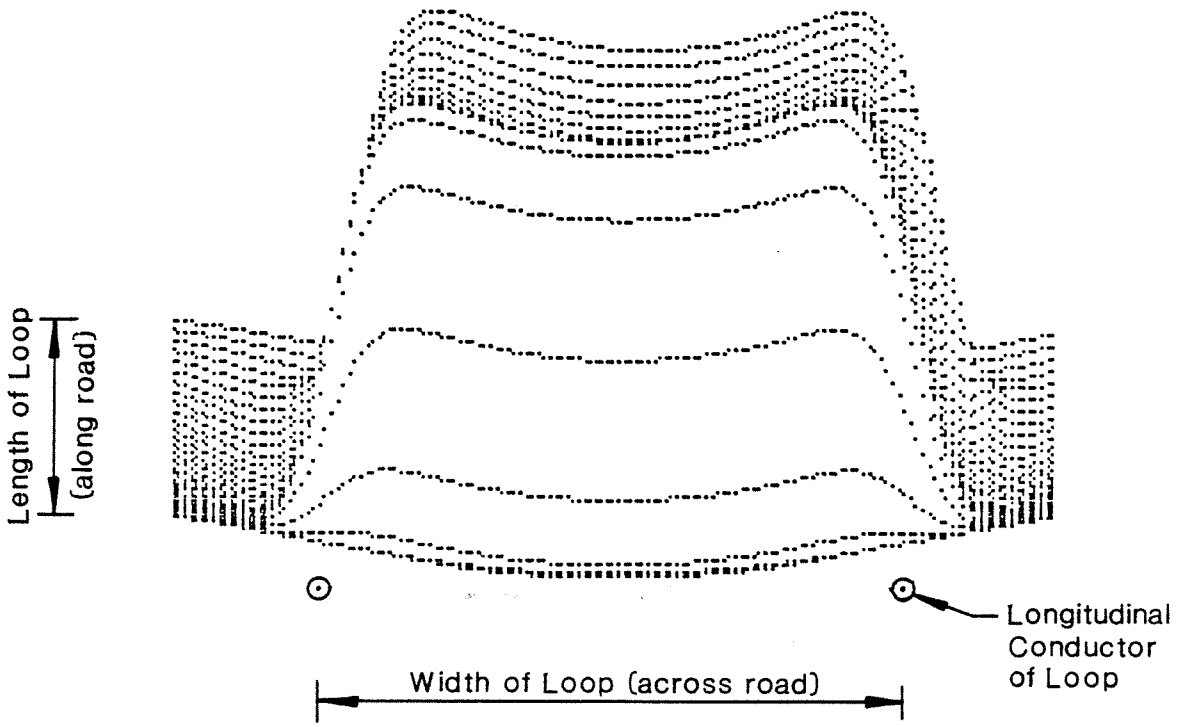

Figure 3.2. Amplitude distribution, depicted graphically, of the vertical magnetic flux density over the square loop at height 0.25m above the loop plane, as in a road. Heights of curves indicate relative flux density above road lanes.

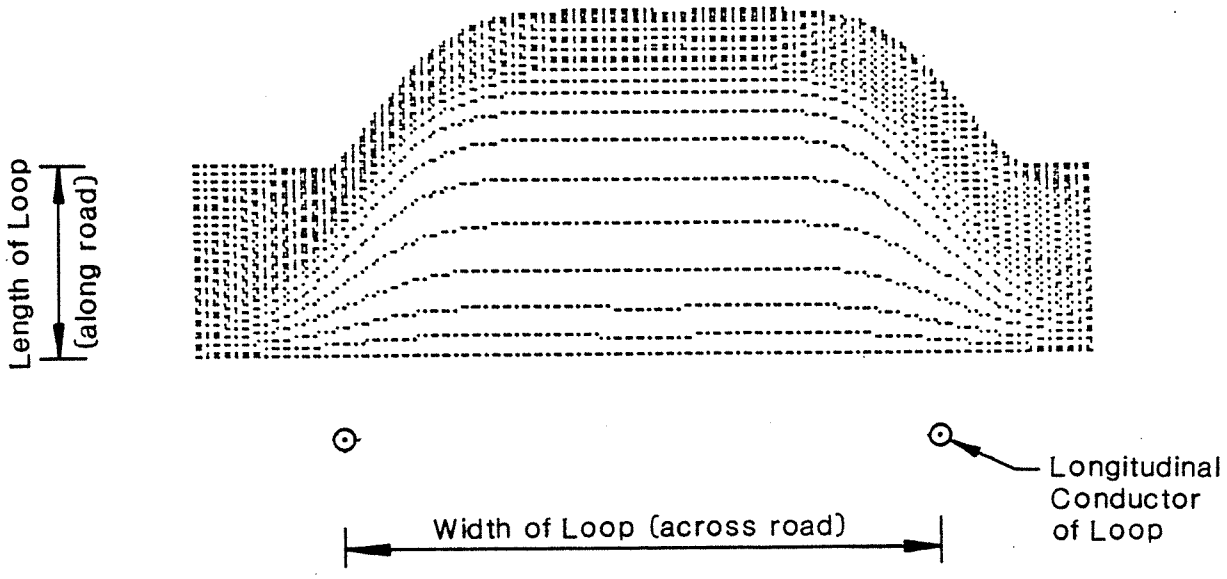

Figure 3.3. Amplitude distribution, depicted graphically, of the vertical magnetic flux density over the square loop of Figure 3.2, at height 0.50m above the loop plane, as in a road. Heights of curves indicate relative flux density above road lanes.

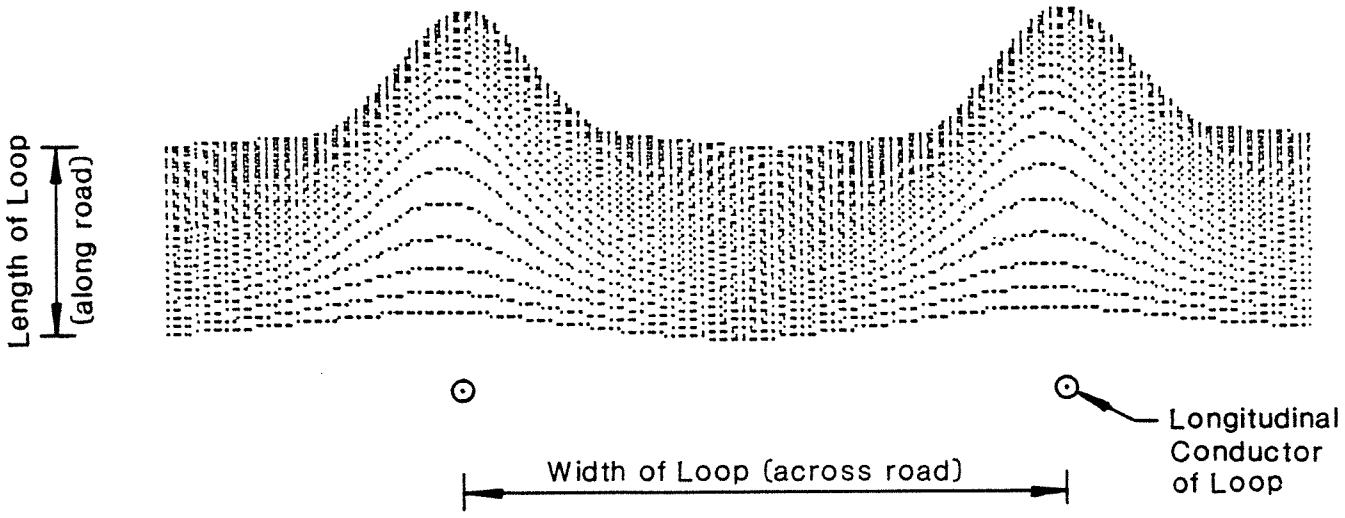

Figure 3.4. Amplitude distribution, depicted graphically, of the cross(-lane) magnetic flux density over the square loop of Figure 3.2, at a height 0.40m above the loop plane, as in a road. Heights of curves indicate relative flux density above road lanes.

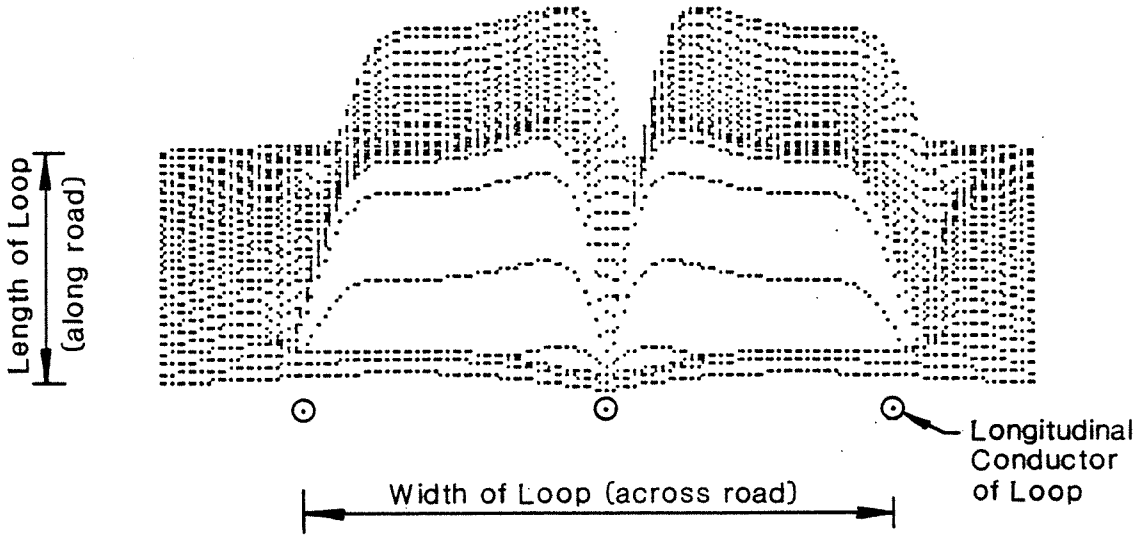

Figure 3.5. Quadrupole loop, 2x2m. Vertical magnetic flux density distribution, depicted graphically, over the loop at a height 0.20m above the loop plane, as in a road. Heights of curves indicate relative flux density above road lanes.

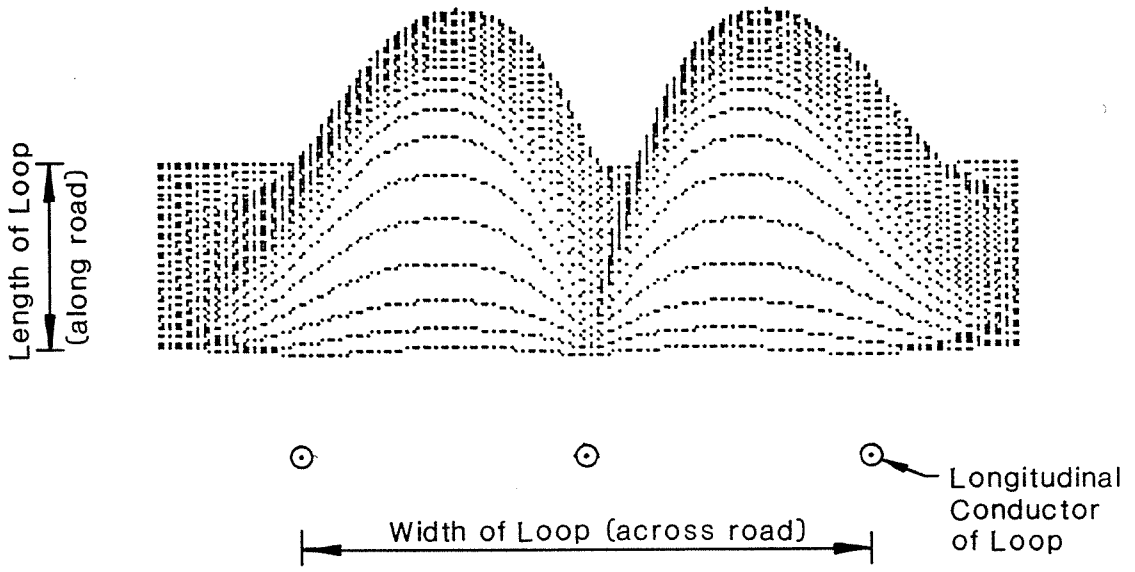

Figure 3.6. Quadrupole loop, 2x2m. Vertical magnetic flux density distribution, depicted graphically, over the loop at a height 0.50m above the loop plane, as in a road. Heights of curves indicate relative flux density above road lanes.

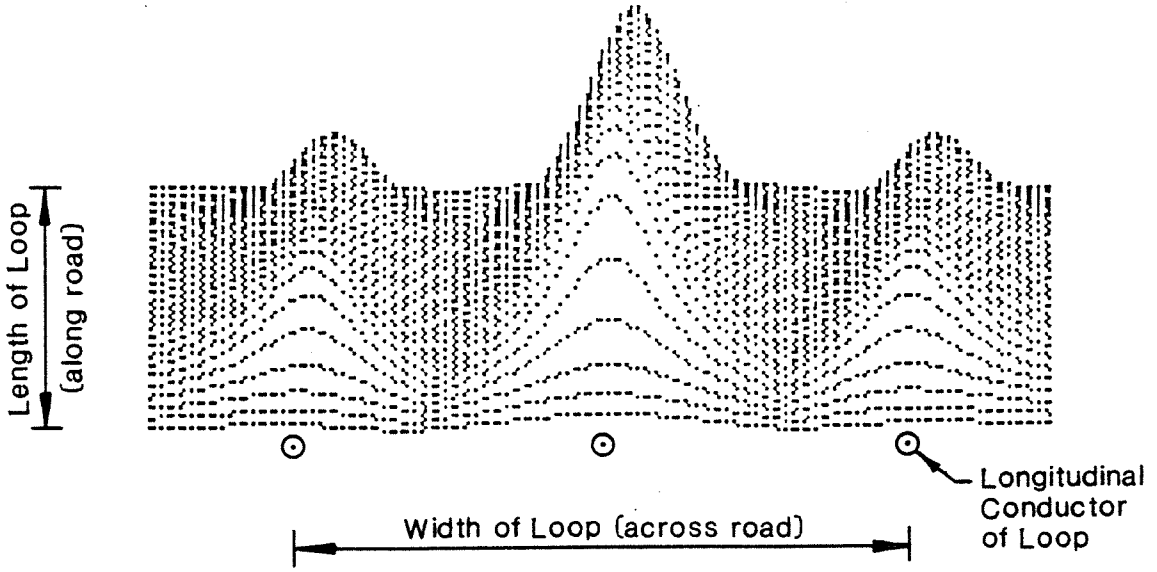

Figure 3.7. Quadrupole loop, 2x2m. Cross(-lane) magnetic flux density distribution, depicted graphically, over the loop at a height 0.25m above the loop plane, as in a road. Heights of curves indicate relative flux density above road lanes.

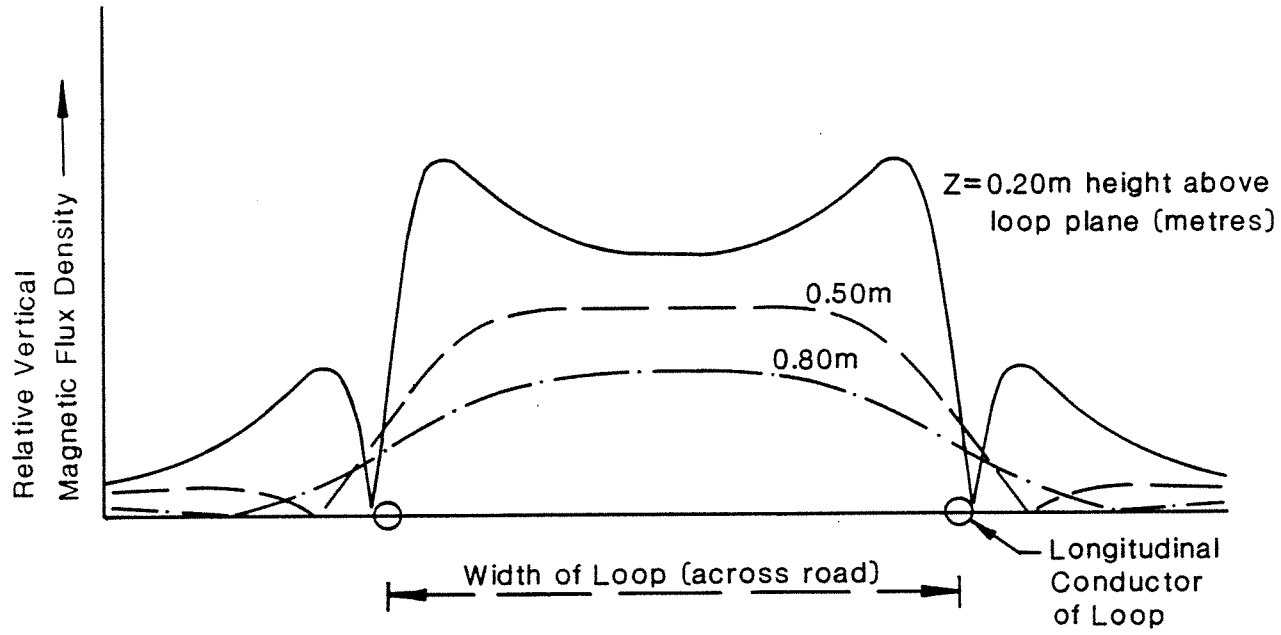

Figure 3.8. Square loop, 2x2m. Vertical magnetic flux density profiles through the mid-section of the loop at heights z = 0.20m, 0.50m and 0.80m above the loop plane. Heights of curves indicate relative flux density at a particular value of "z" above the loop. Circles denote the loop conductors along the road lane.

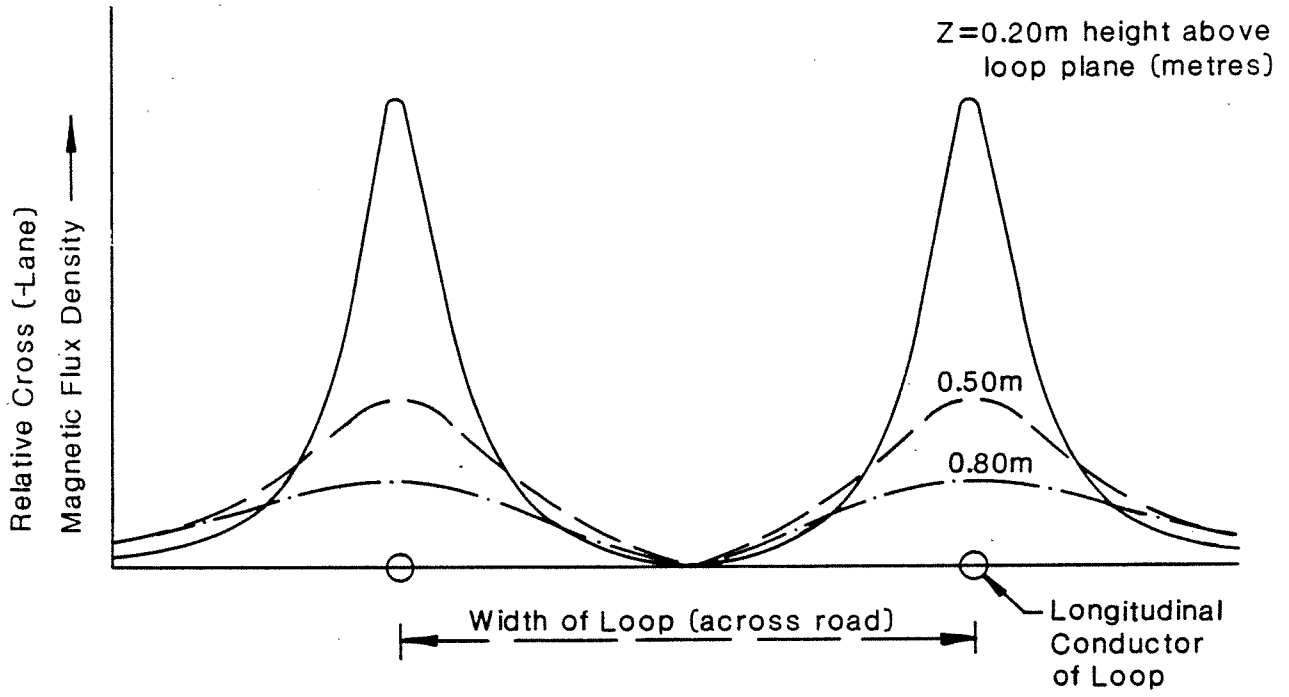

Figure 3.9. Square loop, 2x2m. Cross(-lane) magnetic flux density profiles through the mid-section of the loop at heights z = 0.20m, 0.50m and 0.80m above the loop plane. Heights of curves indicate relative flux density at a particular value of "z" above the loop. Circles denote the loop conductors along the road lane.

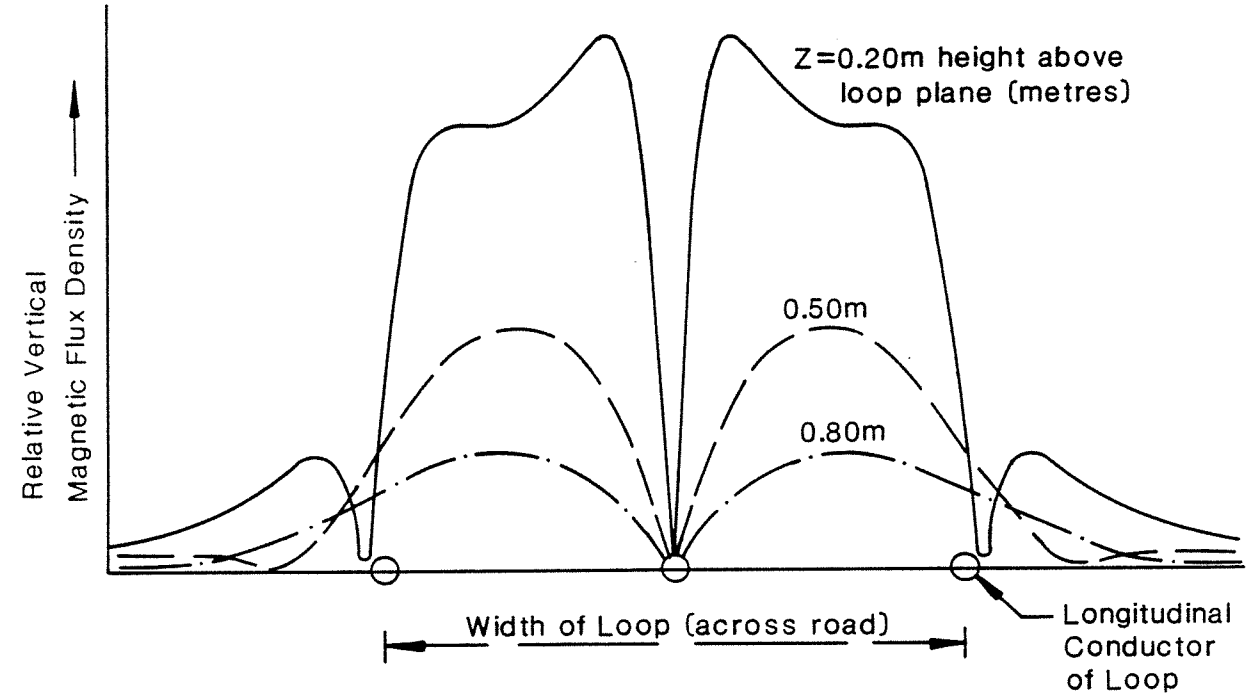

Figure 3.10. Quadrupole loop, 2x2m. Vertical magnetic flux density profiles through the mid-section of the loop at heights z = 0.20m, 0.50m and 0.80m above the loop plane. Heights of curves indicate relative flux density at a particular value of "z" above the loop. Circles denote loop wire sections.

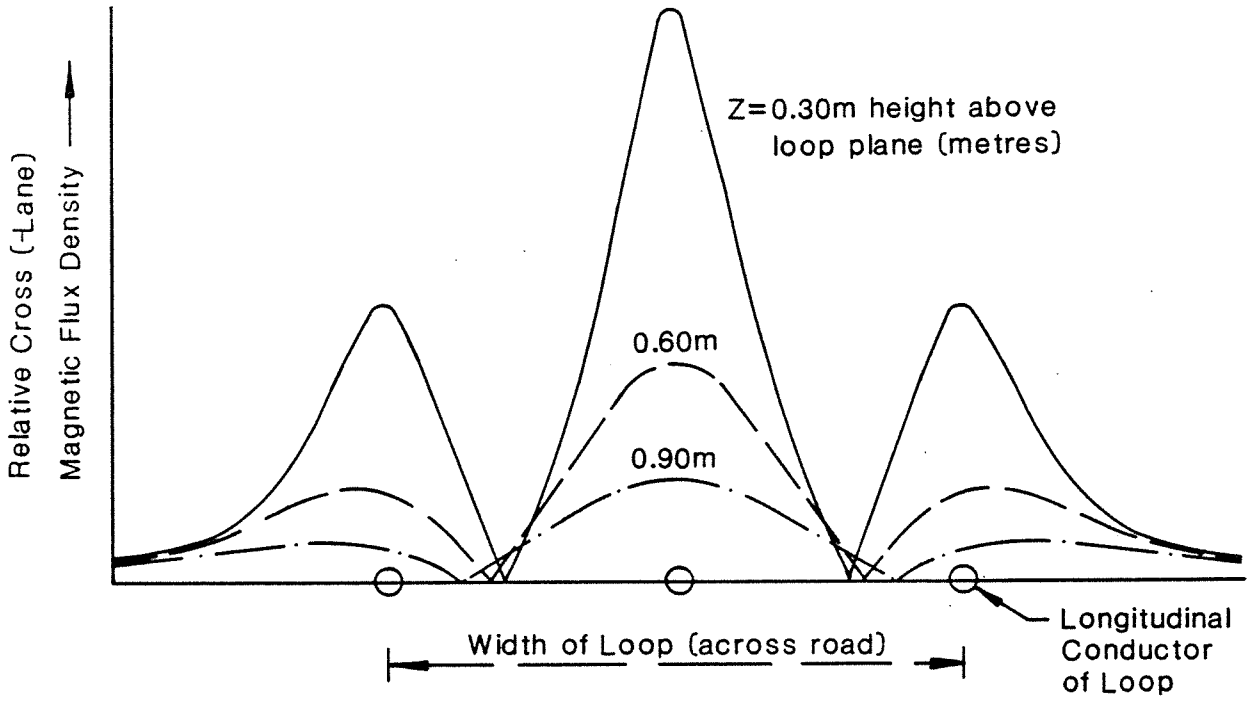

Figure 3.11. Quadrupole loop, 2x2m. Cross(-lane) magnetic flux density profiles through the mid-section of the loop at heights z = 0.30m, 0.60m and 0.90m above the loop plane. Heights of curves indicate relative flux density at a particular value of "z" above the loop. Circles denote loop wire sections.

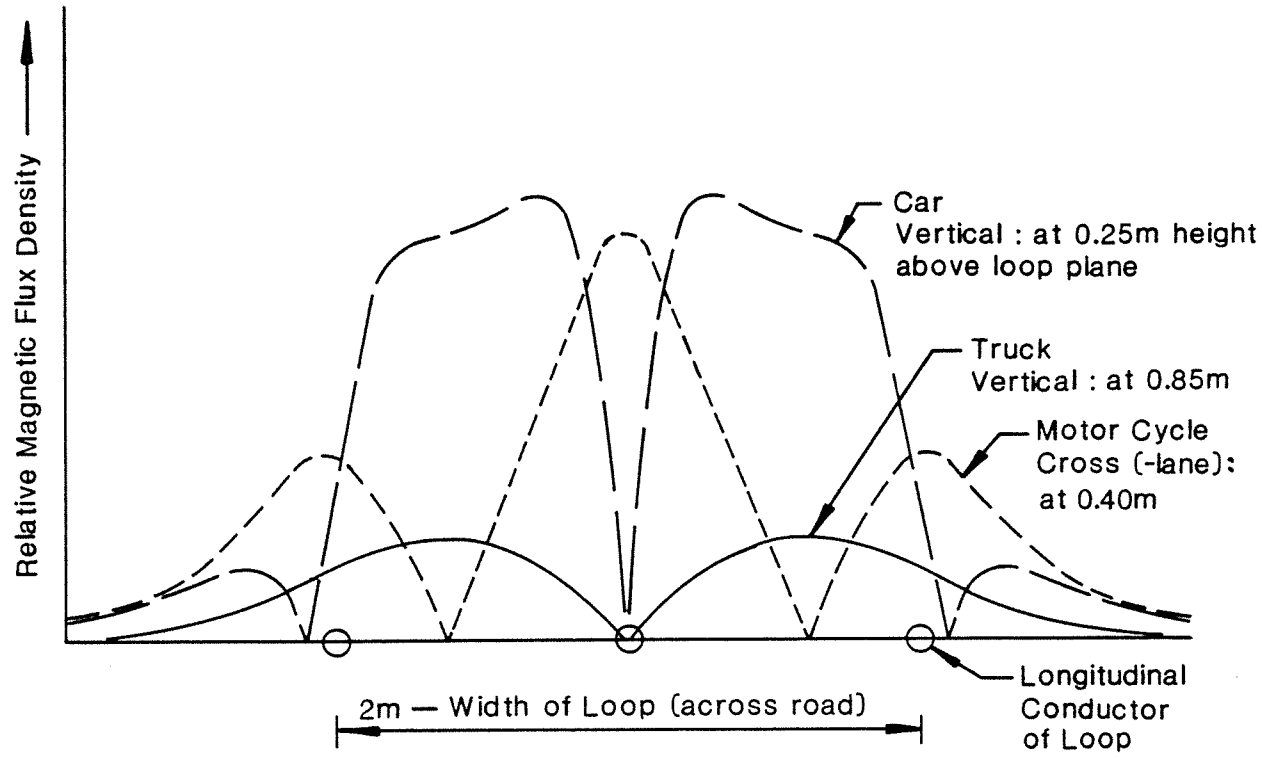

Figure 3.12a. Quadrupole loop, 2x2m. Combination plots of vertical and cross(-lane) magnetic flux density profiles at heights shown, at mid-section of loop.

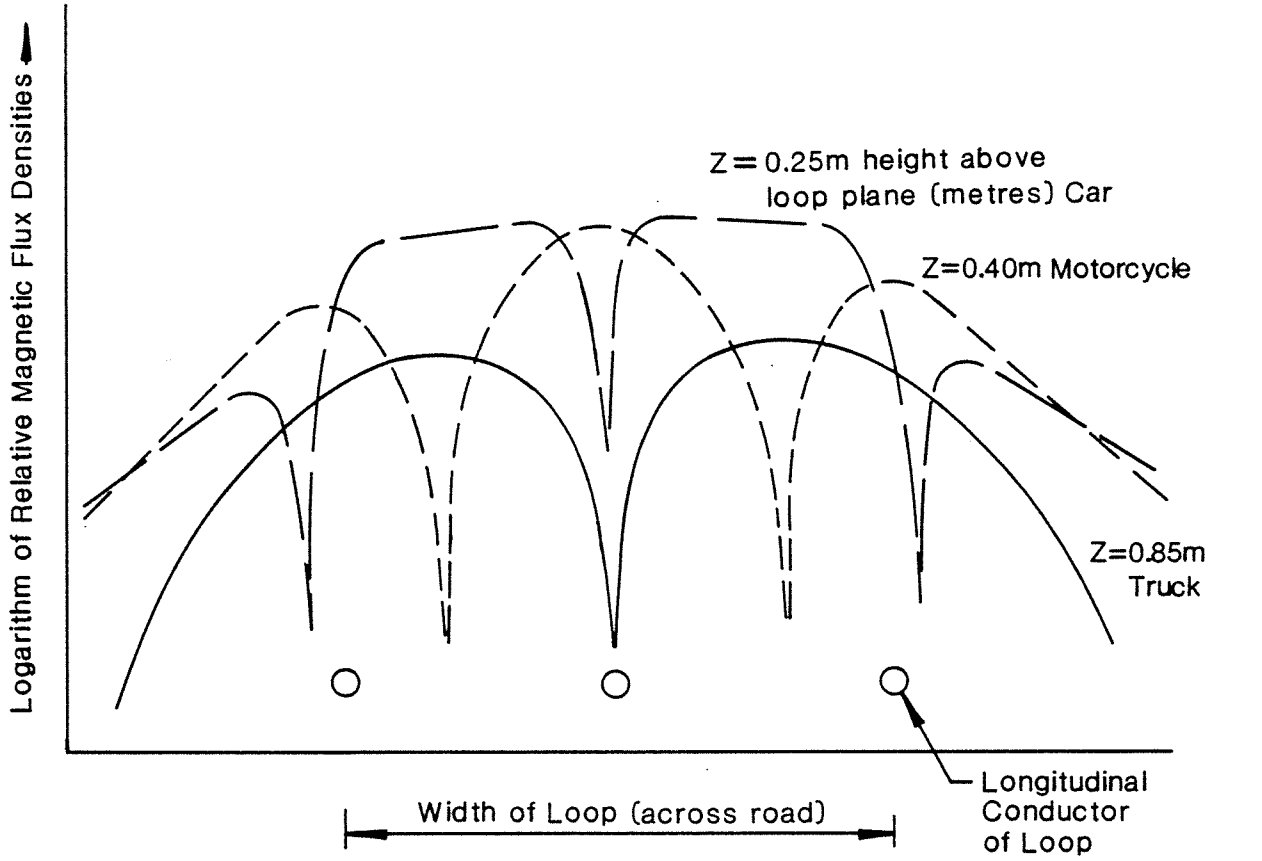

Figure 3.12b. Log-linear plot of Figure 3.12a for comparison with Figure 3.13. Vertical magnetic flux density profiles through the mid-section of quadrupole loop 2x2m, at heights z = 0.25m and 0.85m. Cross(-lane) magnetic flux density profile at height z = 0.40m, at mid-section of loop.

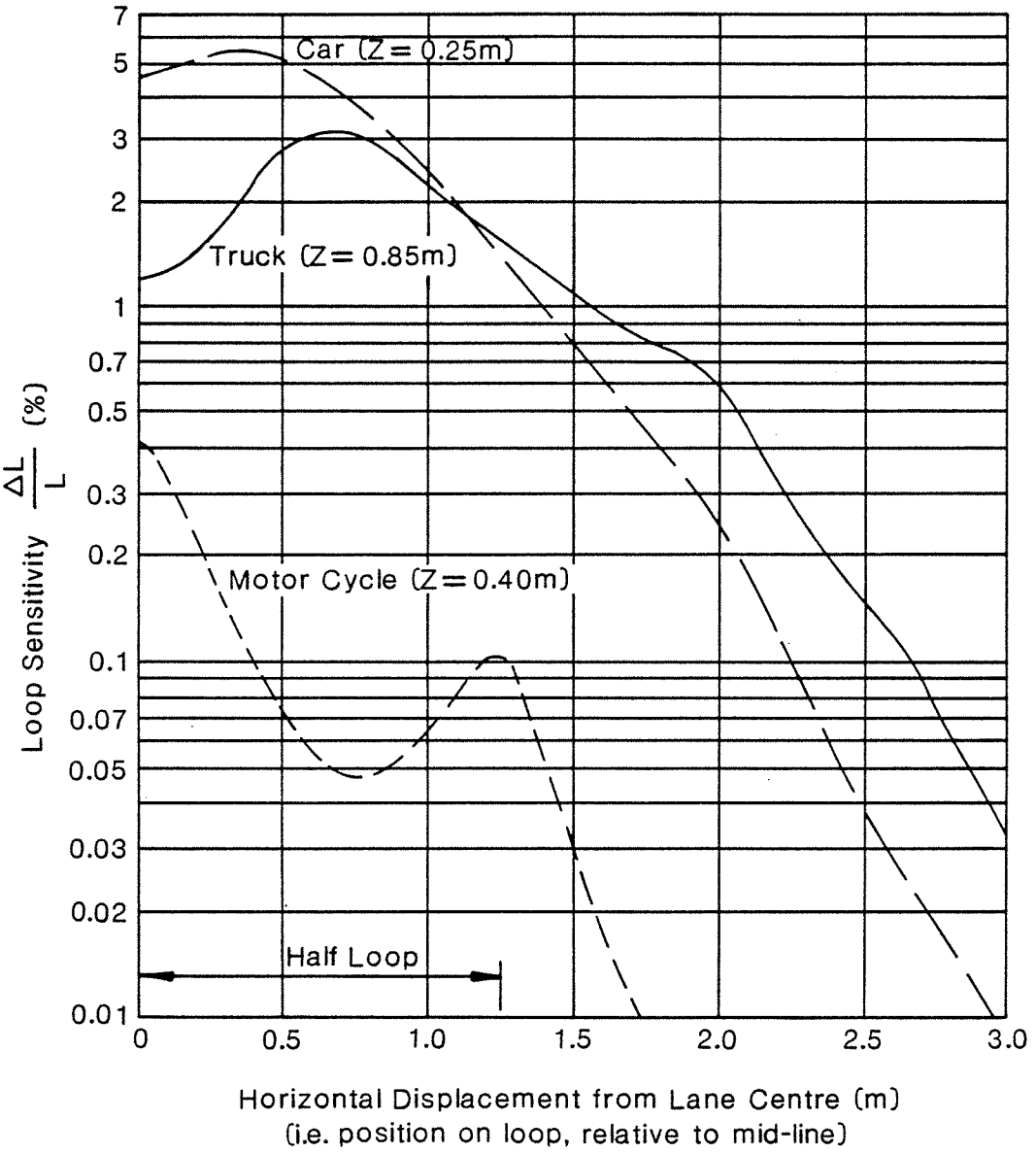

Figure 3.13. Sensitivity curves obtained by Morris *et al.* (1978) for a quadrupole loop. Only half the profile is shown. The sensitivity curves for car and truck correspond to the vertical magnetic flux density profiles at heights z = 0.25m and 0.85m, respectively, of Figures 3.12a and 3.12b. The motorcycle sensitivity curve corresponds to the cross(-lane) magnetic flux density profiles at height z = 0.40m of Figures 3.12a and 3.12b.

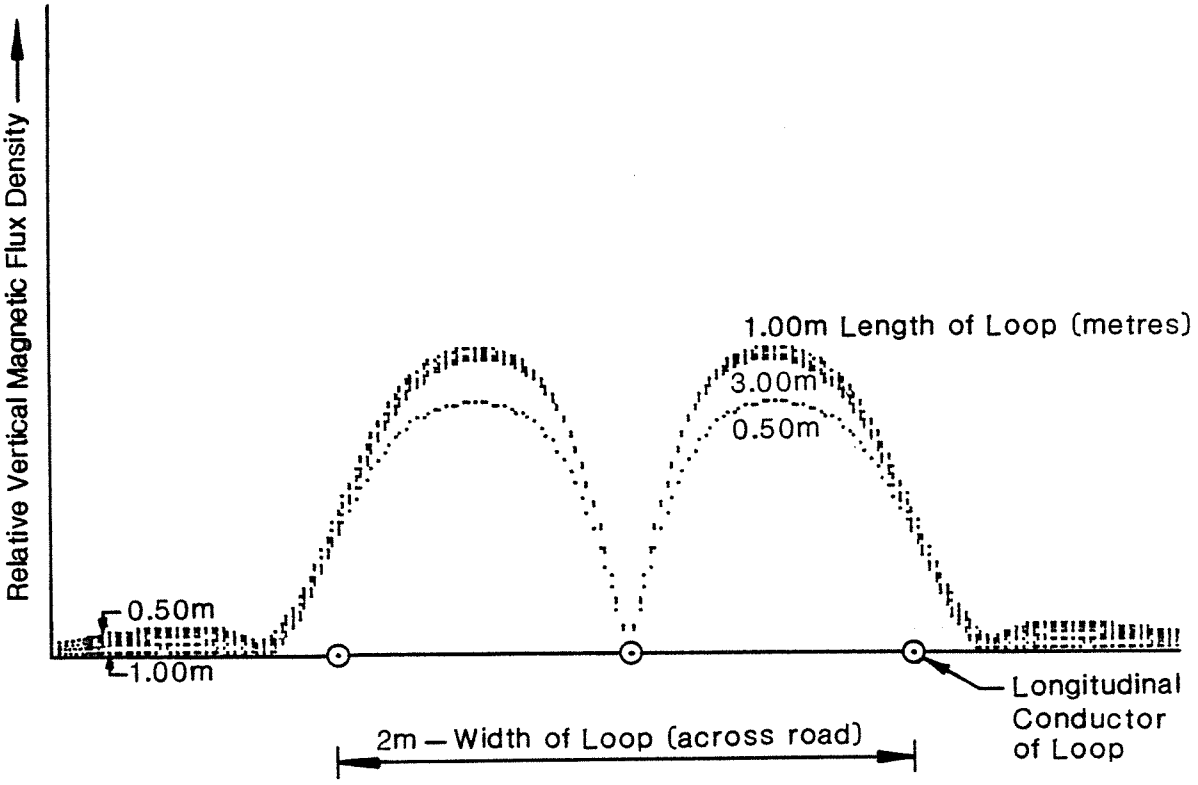

Figure 3.14. Quadrupole loop. Vertical magnetic flux density profiles at the mid-section of the loop. Loop width is constant at 2m across the lane. Parameter is the loop length along the lane from 0.50m to 3.00m, in steps of 0.50m.

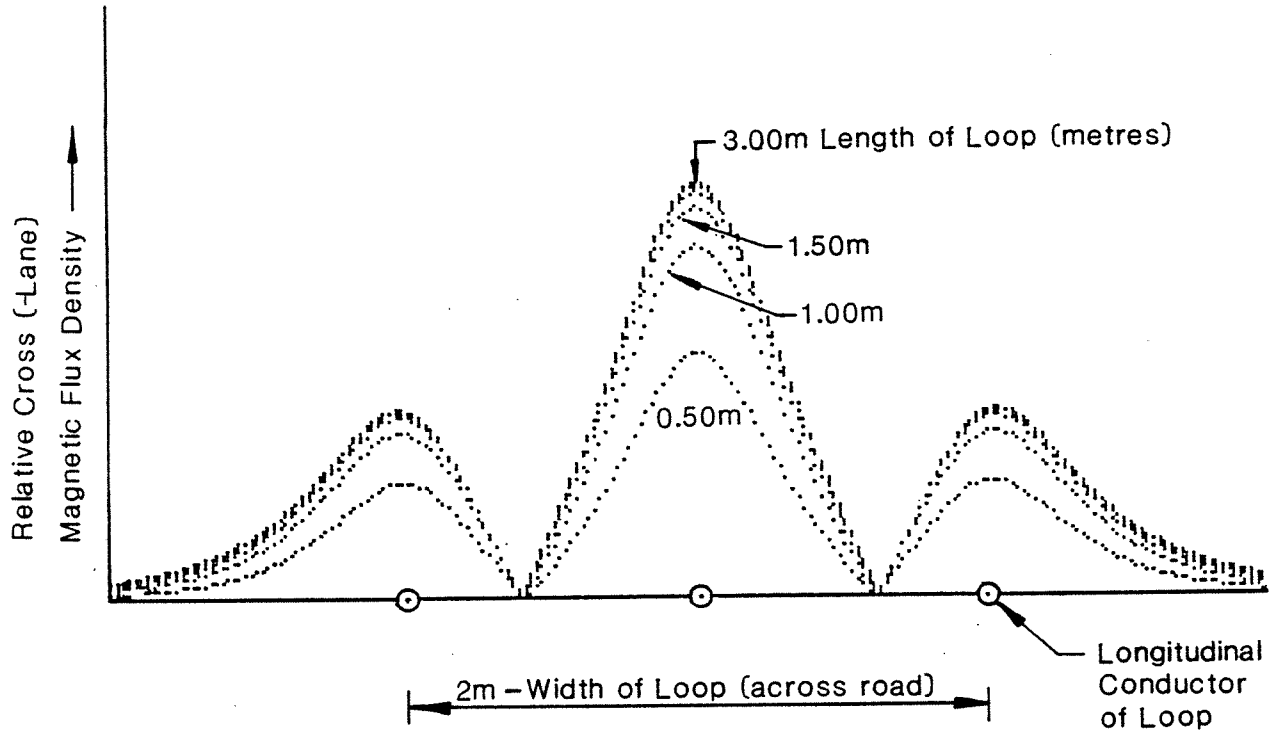

Figure 3.15. Quadrupole loop. Cross(-lane) magnetic flux density profiles at the mid-section of the loop. Loop width is constant at 2m across the lane. Parameter is the loop length along the lane from 0.50m to 3.00m, in steps of 0.50m.

4. FEEDERS OR TRANSMISSION LINES

4.1 Feeders

A feeder or transmission line is used to connect a road loop to the electronic detector. These lines have many forms and dimensions, depending on the particular application. The "transmission line" effects on the operation of a loop become significant in some cases where the line is relatively long and/or the frequency of operation is high. To understand the effects of lines on system operation their relevant properties have been investigated.

4.2 Fundamental Concepts

In an electrically long line, waves will be propagating from the generator to the load (loop) end and, in general, waves reflected from the load end (loop) will be travelling toward the generator (electronic detector) end. Depending on the line length and the frequency of operation, these waves will tend to add to or (partially) cancel each other.

For a single frequency operation, as in loop detectors, the **ratio of the voltage to current waves travelling in the same direction** is constant for a uniform line. This ratio is defined as the "characteristic" impedance of the line.

At any point in a line there will be incident and reflected waves. The ratio of the total voltage to the total current is defined as the "input" impedance of the line at the point. Since the relative phases of the incident and reflected waves vary from point to point, the input impedance to a line will also vary. This is the "impedance transformation property" of the line. If the line is terminated in its correct (characteristic) impedance there will be **no reflected** waves and thus, a **correctly-terminated** ("matched") line will show **no impedance transformation**. Useful lines tend to gave real characteristic impedances (purely resistive). However, when reactive terminations or loads, such as road loops, to a line are used, impedance transformation effects will always be present.

4.3 Characteristic Impedance

The characteristic impedance of a line is determined by its construction, i.e. by the line cross-section and the dielectric material that acts as conductor spacer and insulation. Sometimes the conductors are surrounded by a flexible conducting outer shield. The shield is used to reduce unwanted interference signals from the outside world. An example of a commonly used feeder cable is shown in Figure 4.1.

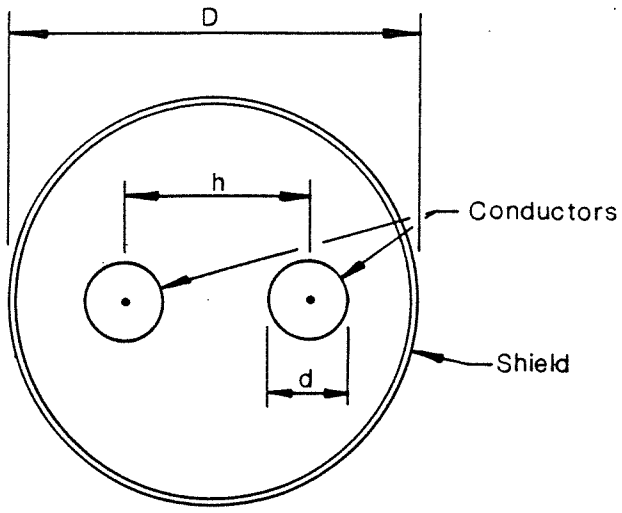

Figure 4.1. Shielded or screened twin conductor line.

An approximate expression for the characteristic impedance of the line is given by Equation 4.1 (ITT Handbook 1977): (Equation 4.1)

$$Z_o = \frac{273}{\sqrt{\epsilon_r}} \log_{10} \left(2 \nu[(1-\sigma^2)/(1 + \sigma^2)] \right) \textit{ ohms}$$

where $v = h/d$, $\sigma = h/D$ and $D >> h$, $h >> d$

ϵ_r is the relative dielectric constant of the interconductor medium.

4.4 Impedance Transformation in a Feeder

Consider a transmission line of characteristic impedance "Z_o" ohms, length "ℓ" metres and terminated in a load of "Z_L" ohms (Figure 4.2).

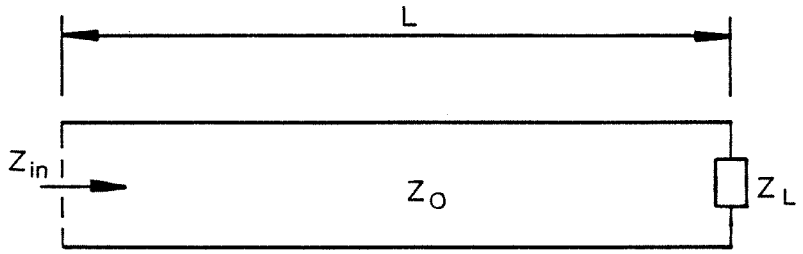

Figure 4.2. Transmission line of characteristic impedance "Z_o" ohms, length "ℓ" metres , terminated in a load of "Z_L" ohms.

At a frequency of f Hz, the impedance seen at input A of this line may be shown to be (Chipman 1968):

$$Z_{in} = Z_o \frac{Z_L \cosh(\gamma\ell) + Z_o \sinh(\gamma\ell)}{Z_o \cosh(\gamma\ell) + Z_L \sinh(\gamma\ell)}$$

(Equation 4.2)

where $\gamma = \alpha + j\beta$ is the "propagation" constant of the line. It is determined by the physical properties of the line, where "j = $\sqrt{-1}$".

$\alpha =$ "attenuation" constant of the line in Nepers/metre. "$\alpha\ell$" is the attenuation in line of length "ℓ" metres long, i.e. $\alpha\ell = \log_e |V_1/V_2|$.

"V_1" is the voltage at a point in line, say, point "A". "V_2" is the voltage at distance "ℓ" metres from "A", in the direction of wave propagation.

$\beta =$ "phase" constant of the line.

$\beta\ell =$ "electrical" length in radians/metre, of the line of length "ℓ"metres, and "β" is the phase constant.

In a lossless line, $\alpha = 0$:

$$\gamma = j\beta$$

(Equation 4.3)

It may be shown that:

$$\beta = \frac{2\pi f}{V_p} = \frac{\omega}{V_p} = \frac{2\pi}{\lambda_g}$$

(Equation 4.4)

where $V_p = \lambda_g f$ is "phase" velocity of waves in line, and λ_g = "guide" wavelength at the frequency of f Hz. Note that for same frequency, the free space and guide wavelengths are not, usually, the same.

"Free space" wavelength "λ" is defined from free space velocity of electromagnetic waves, "c", i.e.:

$$\lambda = \frac{c}{f} = \frac{3 \times 10^8}{f} \ metres$$

Equation 4.2 for the lossless case becomes:

$$Z_{in} = Z_o \frac{Z_L \cos(\beta\ell) + jZ_o \sin(\beta\ell)}{Z_o \cos(\beta\ell) + jZ_L \sin(\beta\ell)}$$

(Equation 4.5)

Note: If $Z_L = Z_o$, i.e. the line is "correctly" terminated, then for any length "ℓ", Equation 4.5 becomes:

$$Z_{in} = Z_o \ (for \ Z_L = Z_o)$$

(Equation 4.6)

Thus, if the loop impedance is equal to the characteristic impedance of the line, then the feeder does not degrade the loop effectiveness. However if, as is normally the case, the magnitude of the loop impedance (a pure reactance) is not equal to the characteristic impedance of the line (usually purely real[3]), then Equation 4.5 shows that impedance transformation takes place along the line. Thus input impedance in the line depends on the line length. This transformation has a graphical solution, the so-called "Smith chart". For details see any book on Transmission Line Theory, e.g. Chipman (1968).

From Equation 4.5 the important parameters in the transformation are:

Z_o — the line characteristic impedance, usually purely resistive,
$\beta\ell$ — the electrical length of the line in radians.

Since

$$\beta\ell = \frac{2\pi f}{V_p} \ell$$

the electrical length depends on:
1. The physical length of the line, "ℓ" metres.
2. The velocity of the electromagnetic wave in the line, "V_p" metres per second.
3. The frequency of operation, "f" hertz.

([3]) See Appendix.

NB: While the frequency of operation may be variable, note that the characteristic impedance of a line is determined at the manufacturing stage and that the available range of values for characteristic impedances is pre-determined and limited.

Representative values for characteristic impedance of feeders in use, at present, with road loops are:

Screened Twin Stereo 0.75mm^2 cable $Z_o \simeq$ 65 ohms
Screened Twin Stereo 0.25mm^2 cable $Z_o \simeq$ 80 ohms

5. THE LOOP-FEEDER SYSTEM

5.1 Introduction

To determine the effect of feeder on the loop-feeder combination, a "sensitivity" factor is defined. This quantity is equal to the relative change in impedance at the input to the feeder (the detector end) divided by the relative change in impedance or inductance at the loop. Thus the sensitivity factor (SF) is a measure of change in system sensitivity caused by the feeder. It is important that, when analysing the effect of feeder, the impedance changes at the loop and at the input to the electronic detector are investigated because a given change in loop inductance caused by a passing vehicle will be transformed by the feeder. In general, the value observed at the detector end will be different from the actual change that may be observed at the loop itself.

The observed value depends on:
1. Line characteristic impedance, "Zo" ohms,
2. Electrical length of the line, "$\beta\ell$" radians,
3. Loop reactance, "X_L".

The undisturbed reactance of the loop is given by:

$$X_L = 2\pi f L_o$$

where π = 3.14159,
f = frequency of operation in hertz (Hz),
L_o = undisturbed loop inductance in henrys (H).

5.2 Sensitivity Factor

For an impedance change at load, "ΔZ_L", the corresponding change in impedance at input to the line, "ΔZ_{in}", may be written as:

$$\Delta Z_{in} = \left[\frac{dZ_{in}}{dZ_L}\right] . \Delta Z_L$$

(Equation 5.1)

Sensitivity or relative change at input to line can be written:

$$Sensitivity \equiv \frac{\Delta Z_{in}}{Z_{in}} = \frac{dZ_{in}}{dZ_L} \cdot \frac{\Delta Z_L}{Z_{in}}$$
$$= \left[\frac{dZ_{in}/Z_{in}}{dZ_L/Z_L}\right] \cdot \frac{\Delta Z_L}{Z_L}$$

(Equation 5.2)

Re-writing Equation 5.2 as:

$$Sensitivity = \frac{\Delta Z_{in}}{Z_{in}} = SF \cdot \frac{\Delta Z_L}{Z_L}$$

(Equation 5.3)

where Sensitivity Factor is defined as:

$$SF = \frac{[dZ_{in}/Z_{in}]}{dZ_L/Z_L}$$

(Equation 5.4)

From Equations 4.2, 5.1 and 5.2:

$$SF = \left| \frac{Z_o Z_L \ (1 - \tanh^2(\gamma\ell)}{[Z_o + Z_L \tanh(\gamma\ell)][Z_L + Z_o \tanh(\gamma\ell)]} \right|$$
$$= \left| \frac{R[1 - \tanh^2(\gamma\ell)]}{[R + \tanh(\gamma\ell)]\ [1 + R\tanh(\gamma\ell)]} \right|$$

(Equation 5.5)

where $R \equiv Z_o/Z_L$.

For a loop having an inductance of "L" henrys:

$$Z_L = j\omega L = j2\pi fL \ ohms$$
$$= jX_L.$$

All these forms are used in various parts of the analysis.

5.3 Lossless Case

For a lossless (or a very low loss) line:

if $\alpha \rightarrow 0$, then $\gamma = j\beta$

Hence, Equation 5.5 for sensitivity factor becomes:

since $tanh(j\beta\ell) = j\ tan\ (\beta\ell)$

$$SF = \frac{Z_o X_L\ (1 + \tan^2(\beta\ell))}{[Z_o - X_L \tan(\beta\ell)]\ [X_L + Z_o \tan(\beta\ell)]}$$

(Equation 5.6)

Here using $Z_L = jX_L$ "reactance" of loop
$= j(2\pi fL)$,

Equation 5.6 may be written, for ease of computation:

$$SF = \frac{(X_L/Z_o)\ .\ (1 + T^2)}{\left[1 - \frac{X_L}{Z_o}\ .\ T\right]\left[\frac{X_L}{Z_o} + T\right]}$$

(Equation 5.7)

with $T \equiv tan(\beta\ell)$.

Equation 5.7 represents the effect of the feeder on the sensitivity of the loop. It is important to note that this is an idealised case as lossy lines in vehicle detection systems will cause a loss of sensitivity and the correct expression of Equation 5.5 must be used.

When $\frac{X_L}{Z_o} tan(\beta\ell) = 1$, (Equation 5.8a)

Equation 5.7 shows that

$SF \rightarrow \infty$, i.e. in an ideal case, sensitivity tends to infinity.

This condition may be re-written as:

$$\left[\frac{2\pi L}{Z_o}\right] .f. \tan \left[\frac{2\pi f}{V_p}\ \ell\right] = 1$$

(Equation 5.8b)

Sensitivity factors greater than unity indicate that a lossless transmission line may actually increase system sensitivity for appropriate frequency, inductance value of loop, "Z_o" of line, and electrical length of line. This last parameter, the electrical length, is given by:

$$\beta\ell = \frac{2\pi\ f.\ell}{V_p} = 2\pi\frac{(\ell)}{\lambda g} radians$$

is a function of the physical length "ℓ", the frequency of operation "f", and the phase velocity of wave in the line "V_p".

Equation 5.7 is plotted for various values of the ratio "X_L/Z_o" against the electrical length of the feeder (Figure 5.1). Notice that for $X_L/Z_o \simeq 1$, SF $\simeq$ 1 for most of the plot.

Thus, the loop inductance, the frequency of operation and the characteristic impedance of the line should be such that the relation:

$$2\pi f L \simeq Z_o$$

(Equation 5.9)

is satisfied. This condition makes sensitivity relatively independent of the line length, and close to the loop's own sensitivity, i.e. sensitivity loss is minimal (Anderson 1970).

Note that high characteristic impedance cable, such as 0.25mm^2 screened twin stereo cable, when combined with low inductance loops and low frequency of operation so that $X_L/Z_o << 1$, will result in a serious loss of system sensitivity.

5.4 Theoretical Results

Computed graphs, for which various parameters were kept constant, are shown in Figures 5.2 to 5.6. For detailed explanations see individual figures.

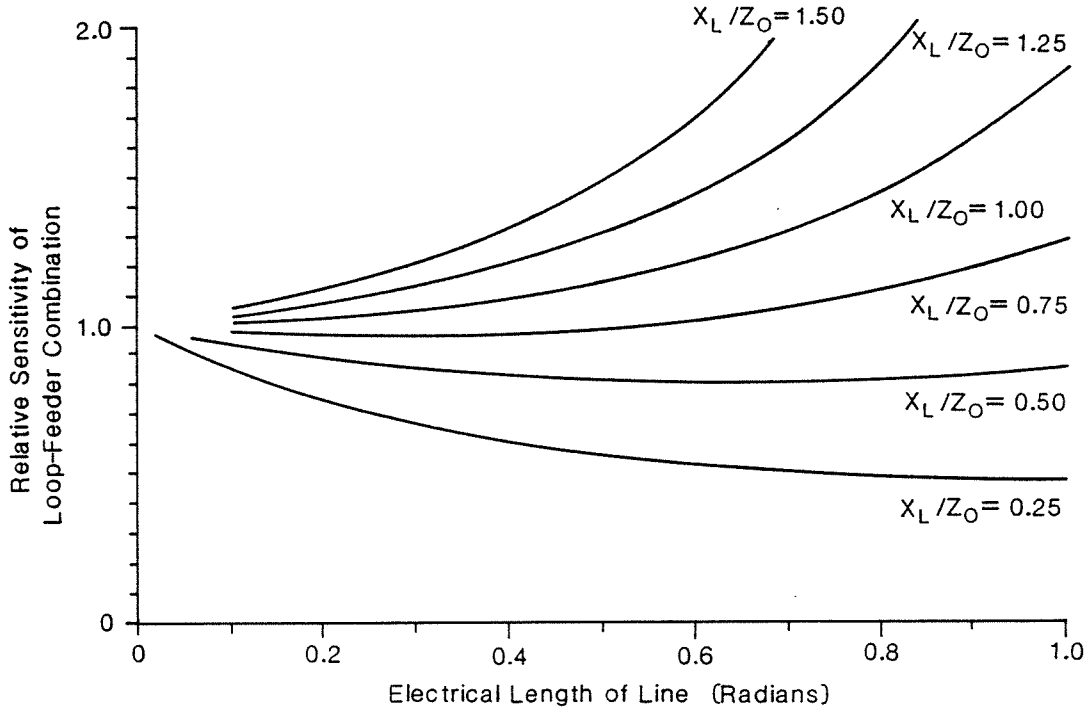

Figure 5.1. Theoretical relative loop sensitivity or response of loop-feeder systems as function of the electrical length of feeder line for lossless line case. The parameter is the ratio of loop reactance "X_L" to the characteristic impedance of feeder line "Z_o".

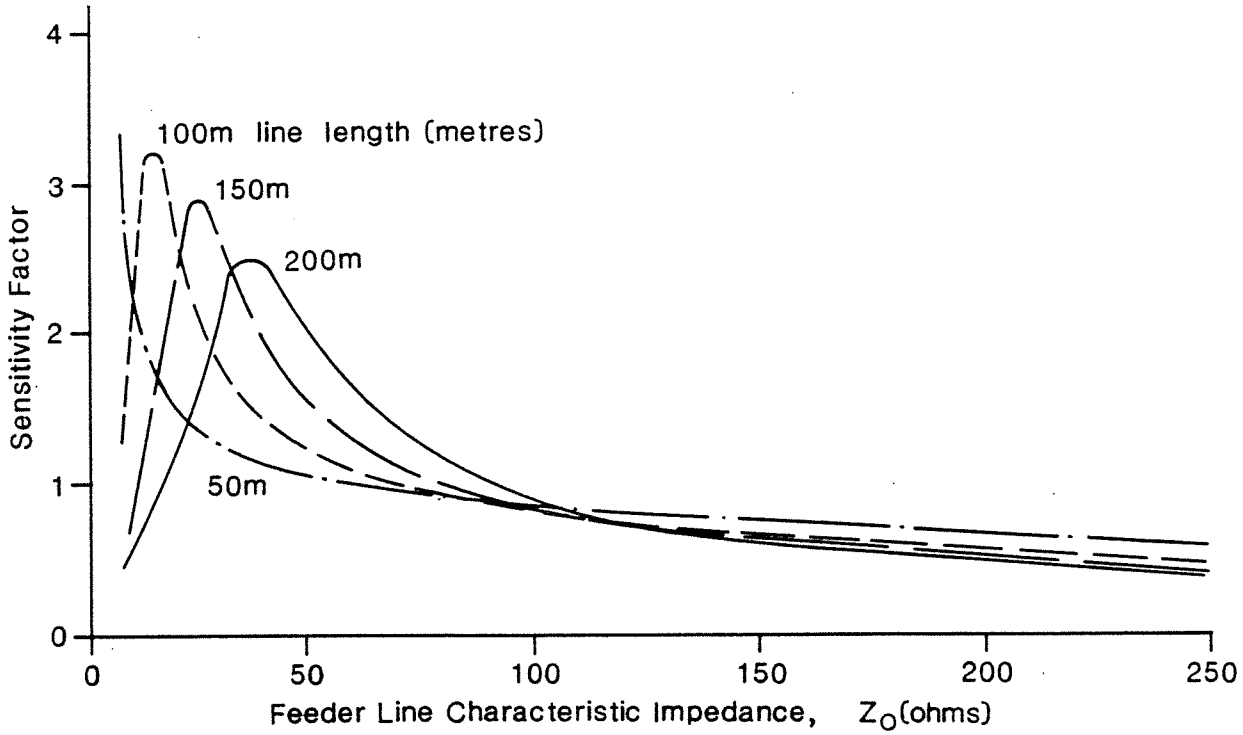

Figure 5.2. Quadrupole loop. Loop sensitivity change as function of the feeder line characteristic impedance. The loop inductance is 138μH and the operating frequency is 60kHz. The parameter is the line length at 50m, 100m, 150m and 200m.

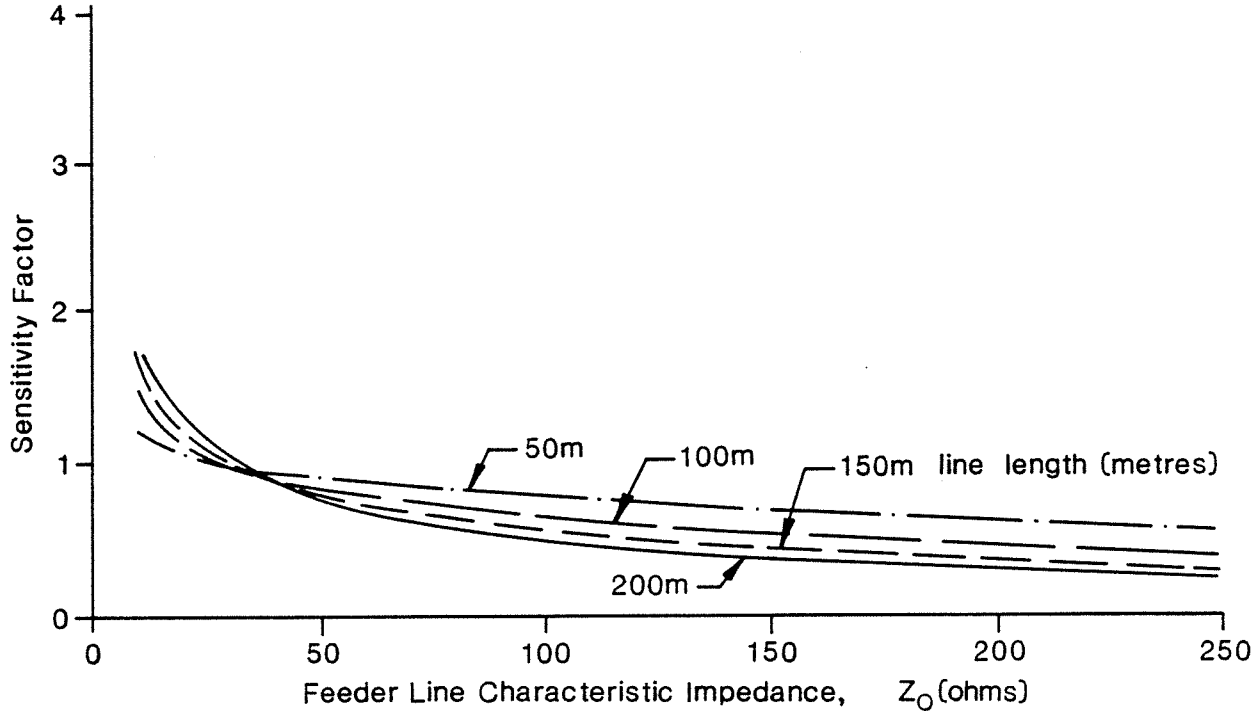

Figure 5.3. Quadrupole loop. Loop sensitivity change as function of the feeder line characteristic impedance. The loop inductance is 138μH and the operating frequency is 30kHz. The parameter is the line length at 50m, 100m, 150m and 200m.

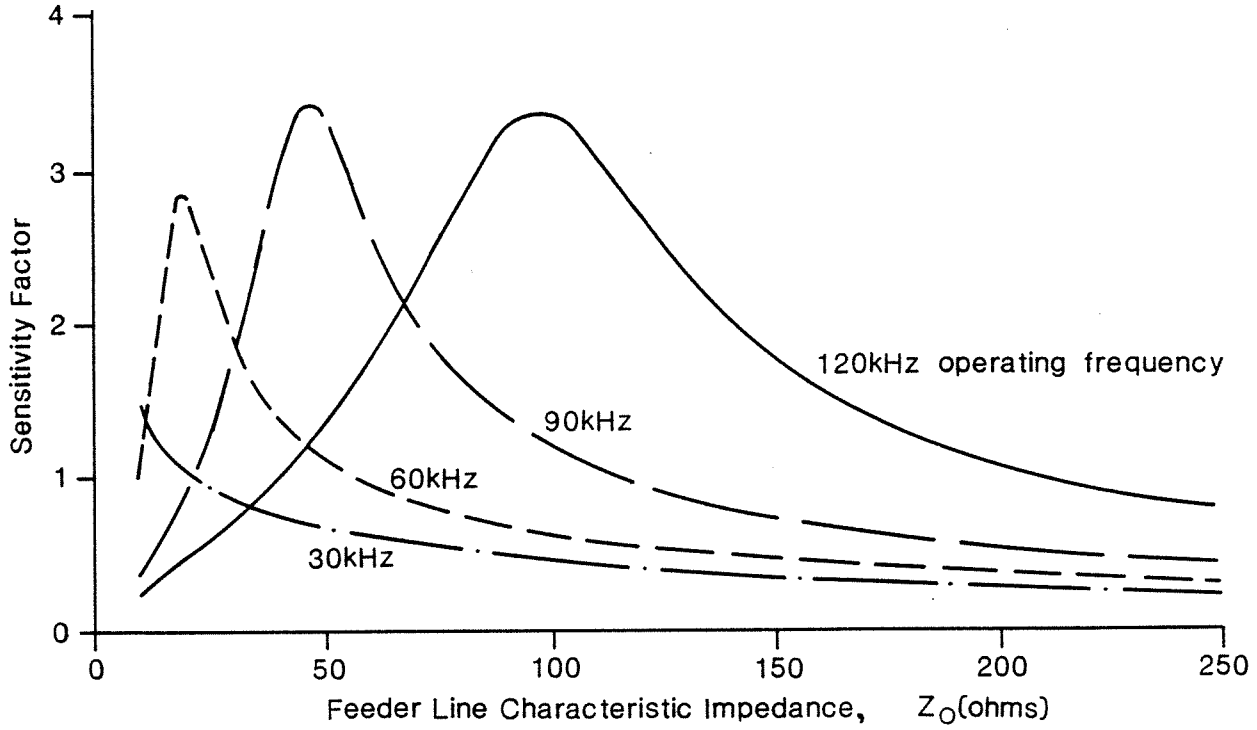

Figure 5.4. Theoretical curves of the loop sensitivity change as function of the feeder line characteristic impedance. The loop inductance is 100μH and the feeder line is 150m long. The parameter is the operating frequency at 30, 60, 90 and 120kHz.

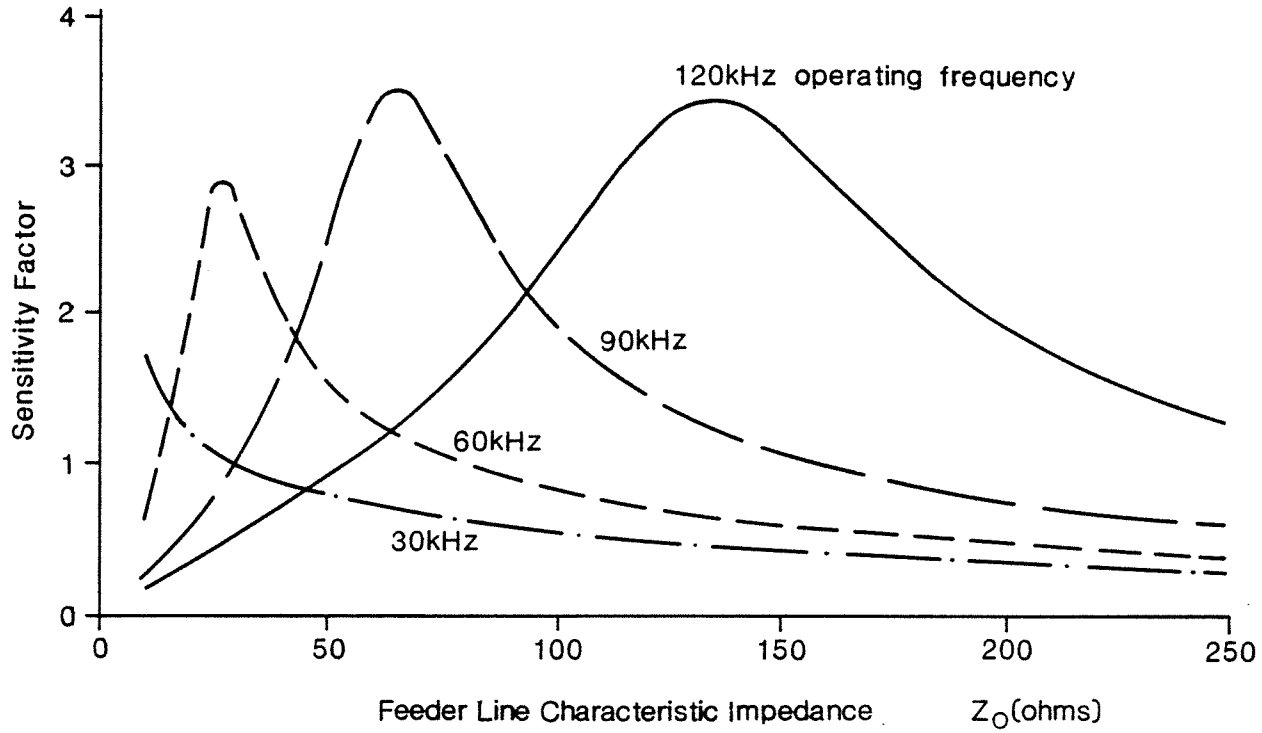

Figure 5.5. Theoretical curves of the loop sensitivity change as function of the feeder line characteristic impedance. The loop inductance is 135μH and the feeder line is 150m long. The parameter is the operating frequency at 30, 60, 90 and 120kHz.

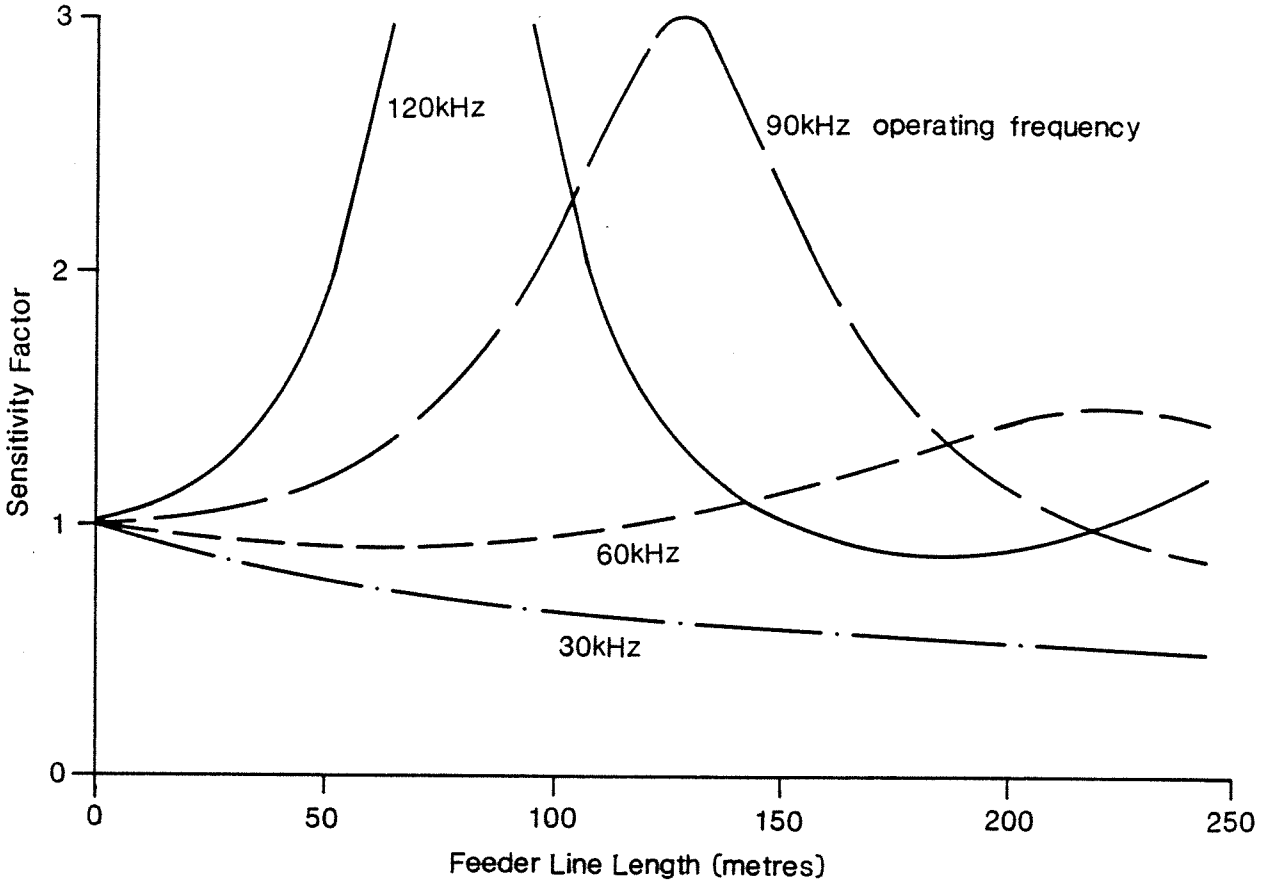

Figure 5.6. Theoretical curves of the loop sensitivity change as function of the feeder length. The loop inductance is 138μH and the line characteristic impedance is 82+jo ohms. The parameter is the operating frequency at 30, 60, 90 and 120kHz.

6. LOOPS OVER METALLIC SCREENS

6.1 Introduction

Road loops used in traffic control mechanisms normally operate in the range of 10kHz to 100kHz. The current flowing in a loop conductor generates a magnetic field in its neighbourhood. The field's spatial distribution depends on the loop geometry, the number of turns and the current through the conductors. Conducting and ferromagnetic objects located within the loop's magnetic field tend to modify the original field. The interaction between a loop and an object is the more pronounced the closer the object is to the loop and it also depends on the relative loop-object orientations. This "closeness" is a function of the loop dimensions and of the operating frequency, i.e. nearness is determined relative to a characteristic dimension of the loop and the wavelength of the operation.

Note that, if as is the case for traffic control use, the wavelength is large relative to the loop dimensions and to the loop-object separation, then the separation relative to a characteristic dimension of the loop is the most important parameter. This fact has been observed in measurements with various-sized and variously shaped loops.

Since the loop is excited by alternating currents, the screen-loop interaction may be caused by:

1. **Eddy Currents**. When vehicles pass above the loop, the time-varying magnetic fields created by the loop excitation induce currents in the screen. Those currents, in turn, produce a secondary or their own magnetic field that interacts with the magnetic field of the loop. Induced currents cause a decrease in flux through the loop.

2. **Reluctance Change**. Ferromagnetic materials decrease the overall reluctance (magnetic impedance) of the magnetic path and, as a result, cause an increase in the flux through the loop.

Note that materials such as steel will produce both of the above effects in varying degrees. The dominant effect depends on the shape of the object and its aspect relative to the magnetic lines of force.

To establish the validity of the model approach, a theoretical study was made of loops placed above a conducting halfspace. The analytical results were approximated from the exact formulation for the case of a **circular loop** over a **conducting halfspace**.

The experimental results were obtained from measurements on circular loops placed over finite slabs. Since the skin([4]) depths at the measuring frequencies were much less than the slab thickness, the actual slab thickness was not considered to be of critical importance.

([4]) Skin or penetration depth is the distance in a medium over which the field attenuates to "e^{-1}", where "e" is the base to the Napierian logarithms.

Note also that the effects of the finite size of screens were not taken into account in the analysis. However, the experimental results indicated that, as long as the diameter of the loop and the loop-screen separation were much less than the dimensions of the screen, the screen may be considered infinite.

6.2 Analysis

For a circular loop of diameter "2a" metres, whose plane is parallel to a conducting halfspace at a distance "b" metres, the expression for the normal flux density in air is approximated from Equation 1 (Tegopoulos and Kriezis 1985):

$$B_z\ (r,\ z) = \frac{\mu_o I}{2a}\int_0^{\infty}\left[\exp\ \frac{(-kb)}{a}\right]\ J_1(k)J_o\left[\frac{kr}{a}\right][\exp\ \left[\frac{-k(z-b)}{a}\right]\ -\ \exp\ \left[\frac{k(z-b)}{a}\right]kdk]$$

(Equation 6.1)

J_n = Bessel function of the first kind and order "n".

The z-axis of the cylindrical co-ordinate system passes through the centre of the loop and the conducting halfspace is at "z=a", the plane of the loop is at "z=0".

The flux density through the loop, $B_z(r,0)$ is then:

$$B_z(r,\ 0) = \frac{\mu_o I}{2a}\ \int_0^{\infty} J_1(k)\ J_o\left[\frac{kr}{a}\right]\ kdk\ -\ \frac{\mu_o I}{2a}\ \int_0^{\infty} J_1(k)\ J_o\left[\frac{kr}{a}\right]\left[\exp\ \frac{(-2kb)}{a}\right]\ kdk$$

(Equation 6.2)

Thus the flux density through the loop is made up of a term related to the loop itself and an additional term related to currents in the slab.

To find the inductance of the loop, first the flux density over the area of the loop needs to be integrated. Finally, use the formula to obtain "L", i.e.

$$\Phi = LI$$

(Equation 6.3)

where Φ is the total normal flux through the loop,
I is the current through the loop wire,
L is the self inductance of loop, a property of loop geometry and the surroundings.

Total flux "Φ" is made up of two terms, since Equation 6.2 can be written:

$$B_z(r,0) = B_0(r,0) - \Delta B(r,0)$$

or:

$$\Phi = \int_A B_z(r,0)dA = \int_A B_0(r_1 0)dA - \int_A \Delta B(r,0)dA,$$

and finally: $\Phi = \Phi_0 - \Delta\Phi$

$$\text{where } \Phi \equiv \int_A B_0(r,0)\ dA \text{ and } \Delta\phi \equiv \int_A \Delta B\ (r,0)dA$$

For the loop inductances in the presence of conducting halfspace, thus:

$$L = \frac{\Phi}{I} = \frac{\Phi_o - \Delta\Phi}{I}$$
$$= L_o - \Delta L$$

(Equation 6.4)

where "L_o" is the "free space" loop inductance,
and "ΔL" is the change in the free space inductance due to presence of the metal slab.

From the above, "L_o" and "ΔL" can now be written as:

$$L_o = \frac{\pi\mu_o}{a} \int_{k=0}^{\infty} J_1(k)k \left[\int_{r=0}^{a} J_o\left[\frac{kr}{a}\right] rdr \right] dk$$

(Equation 6.5)

and:

$$\Delta L = \frac{\pi\mu_o}{a} \int_{k=0}^{\infty} e^{-2kb/a} J_1(k)k \left[\int_{r=0}^{a} J_o\left[\frac{kr}{a}\right] rdr \right] dk$$

(Equation 6.6)

Performing the integrations (Sneddon 1956) inside the parentheses and re-arranging terms:

$$\frac{L_0}{\pi \mu_0 a} = \int_0^\infty J_1^2(k)\, dk$$

These expressions are evaluated (Sneddon 1956, Dwight 1957) as elliptical integrals "E" and "k":

$$\frac{L_o}{\pi a \mu_o} = \frac{2}{\pi k_1} \left[\left[1 - \frac{k_1^2}{2} \right] K(k_1) - E(k_1) \right]$$

(Equation 6.7)

and

$$\frac{\Delta L}{\pi a \mu_o} = \frac{2}{\pi k_2} \left[\left[1 - \frac{k_2^2}{2} \right] K(k_2) - E(k_2) \right]$$

(Equation 6.8)

$$where\ k_1^2 = 1\ and\ k_2^2 = \frac{a^2}{a^2 + b^2}$$

Numerical values may be obtained from Dwight (1957). From Equations 6.7 and 6.8,

"$\Delta L/L_o$" can be plotted as function of "b/a" (Figure 6.1),

Since $L_{slab} = L_o - \Delta L$, it follows that

$$L_o - L_{slab} = L_o - [L_o - \Delta L]$$

$$= \Delta L$$

$$\text{or } \frac{\Delta L}{L_o} = \frac{L_o - L_{slab}}{L_o}$$

i.e. as relative loop inductance change against the normalised loop-screen separation. This plot indicates how the loop inductance changes from its free space value. Sensitivity of the loop is the **inverse** of this function, i.e. the smaller the effect of screen on the loop inductance, the more sensitive the loop is to objects (vehicles) in its field.

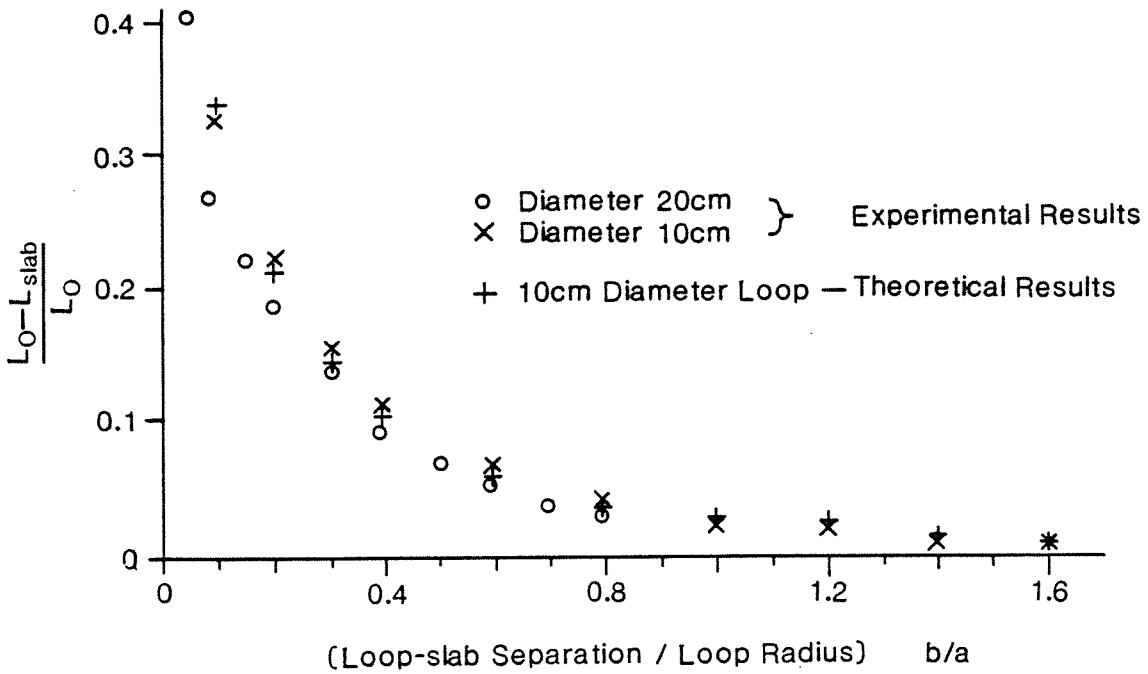

Figure 6.1. Change in the self-inductance of a circular loop above an aluminium slab as a function of the loop-slab separation.

7. CONCLUSIONS

The erratic behaviour of vehicle detection systems used at present in roads around New Zealand may be attributed to environmental factors and to the inability of some of the existing electronic detectors to compensate for these.

The strong correlation that has been established between the spatial sensitivity of a loop and the magnetic flux density distribution about it, is used to determine the detection of objects passing through their magnetic fields.

The sizes and dimension of loops required for optimal detection of vehicles depends on the types of the vehicles. Thus, as the optimum sensitivity of a square loop is at a height of 0.35 times the length of its side, the optimum loop size must be changed to accommodate the various effective heights of vehicles. For example, using the same loop sensitivity, a larger loop is needed to detect trucks and other large vehicles which have chassis at approximately 0.85 metres above the loop plane (in the road). A car has a chassis at average height of 0.25 metres above the loop plane, and would be detected by a smaller loop. Car and truck chassis are horizontal and are detected by the vertical magnetic flux density.

However, to detect bicycles and motorcycles, the problem is compounded by their vertical frames and thus the horizontal magnetic flux density is now of importance. A loop is required therefore that produces a field across the lanes with its optimum at an appropriate vehicle height which, for the representative sample that was measured, is about 0.40 metres.

A compromise between the conflicting requirements for the detection of the various types of vehicles is the quadrupole loop. The optimum dimensions for car and motorcycle detection were found, from theoretical considerations, to be provided by a 2m by 1.75m quadrupole loop. These same dimensions were determined experimentally by workers earlier (about 1978) at the New South Wales Department of Main Roads.

The effect of the feeder on the feeder-loop combination is denoted by the "sensitivity factor", which is a measure of change of sensitivity caused by the feeder. In general, the value of change observed at the detector end of the line will be different from the actual change that may be observed at the loop itself. The sensitivity of the loop-feeder system will not be adversely affected if the magnitude of the loop impedance (pure reactance) is equal to the characteristic impedance of the feeder line. A lossless transmission line (an ideal case) may appear to increase the system sensitivity under a certain set of parameters. However, in practice, with real lines and especially when high impedance lines are combined with low reactance loops (perhaps because low frequency of operation is to be used), the result will be a serious loss of system sensitivity.

The interaction between a ferromagnetic or other conducting object and a loop's magnetic field is the more pronounced the closer the object is to the loop and also relates to its geometry and relative aspect. The measure of "closeness" of an object to a loop depends on the loop dimensions and the operating frequency. At the frequencies of detectors presently used for traffic control, the wavelength is large relative to the typical loop dimension and to the separation between the object and loop. Thus the object-loop separation or, in this case, the height of the vehicle above the loop plane relative to loop size is the most important parameter.

As the presence of conducting and ferromagnetic materials affect the loop sensitivity, reinforcing rods in a road near the loops will, for example, reduce their sensitivity.

Objects made of ferromagnetic materials can increase or reduce the flux through a loop, depending on their geometry and aspect relative to the loop. Thus some may be even "invisible" to the system in appropriate conditions. Changing the content of vehicle construction materials in the future will, no doubt, affect the types of sensors used.

8. REFERENCES

Anderson, R.L. 1970. Electromagnetic loop vehicle detectors. *IEEE Transactions on Vehicular Technology VT-19:* 23-30.

Chipman, R.A. 1968. *Theory and problems of transmission lines.* Schaum Outline Series, McGraw-Hill Book Co., New York.

Dwight, H.B. 1957. *Tables of integrals and other mathematical data.* Macmillan Co., New York.

Langmuir, R.V. 1961. *Electromagnetic field and waves.* McGraw-Hill, New York. 72pp.

Morris, D.J., Hulscher, F.R., Dean, K.G., MacDonald, D.E. 1978. Loop configurations for vehicle detectors. *Australian Road Research Board (ARRB) Conference Proceedings* 9(5): 3-11.

Popovic, B.D. 1971. *Introductory engineering electromagnetics.* Addison-Wesley Publishing Co. Problem G861, p. 279.

ITT Handbook 1977. *Reference data for radio engineers.* 6th edition. Howard W. Sams & Co. Inc., New York.

Sneddon, I.N. 1956. *Special functions of mathematical physics and chemistry.* Oliver & Boyd, Edinburgh. 130pp.

Tegopoulos, J.A., Kriezis, E.E. 1985. *Eddy currents in linear conductivity media.* Elsevier, Amsterdam.

APPENDIX. REAL VERSUS IMAGINARY QUANTITIES AS RELATED TO ALTERNATING CURRENT ANALYSIS

The idea of real and imaginary (or quadrature) entities is a mathematical one, and in electrical engineering it arises from the alternating current technology.

The "phase" difference between the applied potential (voltage) and the resultant flowing current may be expressed in an analytical form using the ideas of real and imaginary quantities. This is directly applicable to sinusoidal signals.

The concept of "phase" may be explained as follows. When a sinusoidal voltage is applied to an electrical component (such as a resistor, an inductor, a capacitor or combinations thereof) then, in general, the peaks of the applied voltage "V", as observed on a monitor, will not coincide with the corresponding, observed, current peak "I". This time difference between the peaks of the two quantities, measured or expressed in electrical degrees or radians is the phase difference between the voltage "V" and the current "I". The phase is related to the time difference "dt" for a wave period "T" by the relation:

Phase difference = dt/T times 360 degrees.

The relation between the voltage and the current at a point in the circuit is given by the generalised Ohm's Law:

$$I = V/Z$$

where "Z" is defined as the impedance at the point.

To show, analytically, the phase difference between "V" and "I", the impedance is made "complex", i.e. it is made up of real or in-phase component and of an imaginary or quadrature component. Thus, if the voltage "V" and current "I" are in phase, then the impedance is "purely real", i.e. it has no "imaginary" component. If the two quantities "V" and "I" are 90 degrees out of phase, then the impedance is "purely imaginary" or "purely reactive" and it has no real component.

In general, the phase difference between "V" and "I" is none of the above two extremes and so the impedance is "complex" i.e. it has both "real" and "imaginary" parts. Note that an ideal or lossless loop is a pure reactance or, equivalently, its impedance is purely imaginary.